Tetrahedron 67 (2011) 6901–6916

Contents lists available at ScienceDirect

Tetrahedron

journal homepage: www.elsevier.com/locate/tet

Three-component conformational equilibria of some flexible pyrrolidin-2-(thi)ones in solution by NMR data (δ_C, δ_H, and $^nJ_{HH}$) and their DFT predictions: a confrontation of different approaches☆

Ryszard B. Nazarski [a,*], Beata Pasternak [a,b], Stanisław Leśniak [b]

[a] Laboratory of Molecular Spectroscopy, Faculty of Chemistry, University of Łódź, Tamka 12, 91-403 Łódź, Poland
[b] Department of Organic and Applied Chemistry, Faculty of Chemistry, University of Łódź, Tamka 12, 91-403 Łódź, Poland

ARTICLE INFO

Article history:
Received 27 January 2010
Received in revised form 15 June 2011
Accepted 24 June 2011
Available online 30 June 2011

Keywords:
IEF-PCM and COSMO solvation model
Karplus equation
GIAO method
WC04, WP04, and B2PLYP functionals
Scaling factor
London dispersion forces
Grimme's DFT-D3
Conformational distribution
DP4 'probability' analysis

ABSTRACT

Three standard gas-phase B3LYP/6-31G(*d*) methods of the analysis of δ_C, δ_H, and J_{HH} NMR data for solutions initially used for the title γ-lactams **1a**–**c** led to conflicting findings on fractional populations ηs of their fast interconverting conformers **A**–**C**, which were also inconsistent with energy data. In order to find the source(s) of these discrepancies, several additional DFT computations were carried out at the double- and triple-zeta theory level with simultaneous modeling of the solutions in explicit solvents with the COSMO or IEF-PCM technique. The WC04/WP04 functionals and IGLO-II (or IGLO-III) basis set were applied for predicting δ_C/δ_H, and J_{HH} data, respectively. The limits of efficiency and accuracy of a few current NMR-oriented computational protocols were determined by their specific use to the main forms of **1a**–**c** treated as test cases. Thus, an unreliability of the modified Karplus-type equation for this purpose was shown. In turn, only the use of DFT-D3 corrections for the attractive van der Waals dispersion interactions (London forces) not present in conventional DFT, to Gibbs free energies (ΔG) estimated for the forms **A**–**C** of **1a**–**c** in solution, yielded energetics and so populations (η_Gs) compatible within ±15% (only ±2%, for **1a**) with the best results found by considering the ^{1}H NMR data. These η_Hs were found by a linear regression of GIAO-predicted δ_H sets reproducing experiment in the best way (r^2>0.9996, for **1a** and **1b**, r^2=0.9970, for **1c** with strongly degenerated δ_Hs). As for η_Js, they permitted only for evaluations of the ratios (**A**+**B**)/**C**, excepting sufficiently differentiated J_{HH}s (**1b** in acetone). In contrast, an application of δ_Cs for assessing η_Cs was unsuccessful. Selected findings were finally compared with the DP4-probability results (η_{DP4}s) and fairly good agreement was found. The greatest divergence in ηs exists for the C=S bond-containing object **1b**, what suggests a large effect of the intramolecular London forces on its structure and properties. The present results should be useful guidelines for NMR studies on the other multi-conformer systems in rapid equilibrium between more than two energetically feasible forms.

1. Introduction

Modern high-resolution NMR spectroscopy is an extremely powerful tool for investigating the stereochemistry and dynamics of organic entities, especially carbo- and heterocyclic, in particular, when elucidating the relative or absolute configuration and/or assessing the most probable shape of such molecular species in solutions. Nowadays, these possibilities became considerably enhanced for common spin-1/2 magnetic-active nuclei *K*, by using two supporting methods of current computational chemistry, i.e., GIAO (gauge-including atomic orbital)[1] predictions of the nuclear magnetic shielding constants, σ_Ks, and density functional (DFT) calculations of the indirect nuclear spin–spin coupling constants often referred to as J_{KL}-couplings.[2] The former of these two fundamental NMR physical observables—more precisely, correlated chemical shifts, δ_Ks—are especially sensitive to the chemical environment of nuclei *K* and conformational mobility of the analyzed molecules, thereby providing an insight into their local functionality, stereostructure and occurring dynamic processes.

Structural studies are usually difficult for flexible molecules existing in solutions as equilibrium mixtures of several non-equivalent fast interconverting conformers. The individual forms present in such dynamic equilibria differ in their spectroscopic properties and, so, the measured values of both NMR parameters mentioned above are the weighted averages over total conformer populations. Hence, the overall[3] (i.e., superimposed in the time)

☆ Physical image versus molecular structure relation, Part 15. For Parts 13 and 14, see Refs 73 and 3b, respectively.

* Corresponding author. Tel.: +48 42 635 5615; fax: +48 42 665 5258; e-mail address: nazarski@uni.lodz.pl (R.B. Nazarski).

0040-4020/$ – see front matter © 2011 Elsevier Ltd. All rights reserved.
doi:10.1016/j.tet.2011.06.095

multi-component conformations of this kind of entities are only examined in such cases, even at extremely low temperatures. In consequence, determination of the shapes of distinct coexisting conformers and, especially, their contributions to ensembles of all of the possible forms can be particularly challenging.[3,4]

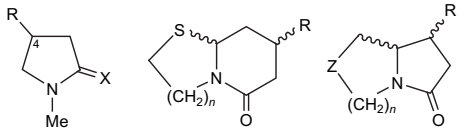

1a R = Ph, X = O
1b R = Ph, X = S
1c R = C(O)Ph, X = O

2 R = aryl
n = 1 or 2

3 R = Ph or CO_2Me
Z = CH_2 or O or S
n = 1 and/or 2

As part of our continuing NMR studies on mobile open chain,[3a] cyclic,[5] and macrocyclic[3b,c,6] systems, we have investigated the flexibility and overall[3] (time-averaged) molecular geometries of 1-methyl-4-substituted-pyrrolidin-2-(thi)ones **1a**–**c** possessing a C-4 substituent [R=phenyl or benzoyl, –C(=O)–Ph],[7] whose conformational features have not been reported to date. Preliminary data[8] indicated that these entities must be considered as flexible molecules, in marked contrast with the previously analyzed relatively rigid fused-ring diastereomeric bicyclics **2**[9] and **3**,[7c] having a bridgehead nitrogen atom in the six- or five-membered lactam unit. Indeed, all diagnostic NMR chemical shifts evaluated from the ^{1}H and ^{13}C NMR spectra of γ-(thio)lactams **1** were recognized as averages (strictly, population-weighted mean values) of the spectroscopic molecular parameters associated with pertinent conformer mixtures of the three rapidly interconverting isomeric forms. Fortunately, a complementary structural information was also available experimentally via the mean values of proton–proton couplings, $^nJ_{HH}$, which are operative within the heterocyclic moieties of these molecules.

With such structurally interesting compounds **1** in our hands, it was the opportunity to perform an exploration of possibilities of the use of various present-day NMR-focused calculational methods for the sake of conformational analysis of the mobile molecules. Quantum-mechanical (QM) ab initio or DFT computations have been applied to an interpretation of NMR spectra of organic systems for more than a decade.[4a,e,10] Every time, the theoretically predicted sets of spectroscopic data are compared against those measured experimentally. Initially, a GIAO ansatz-based calculation of ^{1}H and, especially, ^{13}C chemical shifts was mainly used for this purpose—this technique has been pioneered by Forsyth[4a] and Bifulco.[10] The latter author and his co-workers also modified and extended, to the multiple conformer equilibria,[4f] the J-based analysis originally devised by the Murata group.[11] This important area of the determination of relative configurations in acyclic carbon units of the organic systems, especially natural products, based on a combination of NMR data ($^3J_{HH}$ and $^{2,3}J_{CH}$) and computational methods was tested and reviewed several times.[12]

For a much more computationally demanding J_{KL}-coupling prediction,[2,13] this approach was inter alia used as a separate tool in the analysis of the extremely mobile molecules cyclopentane and tetrahydrofuran.[14] Usual statistical estimates applied for quantifying the agreement between theoretical and experimental NMR data were recently critically discussed and extended for the GIAO-predicted and measured δ_Ks (where K=C and/or H), by considering a long series of diastereomeric structures.[12c,e] Especially, the recent work by Smith and Goodman is worth mentioning here, because the proposed by them DP4 'probability' analysis[12e] solves a problem when only one set of experimental chemical shifts is available to which one possible diastereomeric structure out of many must be assigned. Important effects of use of different levels of electronic-structure theory at various stages in NMR calculations were also studied.[4a,13a,d,15]

In the context of the literature reports outlined above, we were particularly interested in examining the limits of efficiency and accuracy of selected NMR-oriented computational protocols specifically applied for the title compounds **1** treated as test mobile cases, especially in view of our recent δ_C-based results on highly flexible multi-conformer tetraazamacrocycles.[3b,c] Accordingly, solution NMR parameters extracted from the experimental spectra of γ-(thio)lactams **1** were thoroughly considered versus their theoretical values DFT computed for all their lowest energy forms **A**–**C** (i.e., global minima and two local minima, respectively) located in the gas phase[16] and in two PCM[17] self-consistent reaction field (SCRF)-simulated solutions of **1b**, by a rational use of the linear regression analysis.[2b,3,4a,c,e,g–j,10,15a–e,18] The most widely employed theoretical framework for the calculation of geometries and molecular properties of common organic systems was applied, consisting of the B3LYP hybrid functional[19] (as one of the more successful DFT tools for predicting NMR quantities)[15j] paired with a Pople's 6-31G(d) basis of double-ζ (DZ) valence quality. In fact, this functional-basis set combination, employed in numerous GIAO calculations of δ_Hs and δ_Cs, gives, in general, good results.[3b,4a,e,7c,10,15b,20]

Unexpectedly, three different NMR-focused computational methodologies based on an independent DZ-level DFT treatment of δ_C, δ_H, and J_{HH} data, respectively, led to strongly incompatible findings about the fractional conformer populations, μ_Xs (where X = C, H or J) of the title systems **1a**–**c** in solution. Moreover, more advanced GIAO B3LYP/6-31G(d,p) NMR calculations,[12c–e,15d,18e] carried out at geometries acquired at the same level of approximation,[2b,4i,12d,13d,15b,d,18e,21] gave even worse results on the forms **A**–**C** of the smallest object **1a** under study. As already said, our training entities **1** were found to be highly flexible molecules in dynamic equilibrium between their conformers of roughly similar energy. However, only J_{HH} computations with an IGLO-II[22] basis set gave the qualitative conclusions (in particular, for **1a** and **1b**) intelligible in the light of standard gas-phase B3LYP/6-31G(d) energy data and the trends found in two PCM simulations of explicit solutions of **1b**.

In an effort to better understand these inconsistencies, we performed several series of additional DFT calculations on geometries of all key forms **A**–**C** of systems **1a**–**c** as well as the evaluation of their NMR and, especially, energetic properties (including adequate thermal and London dispersion corrections) for $CHCl_3$ solutions. Accordingly, various triple-ζ (TZ) fully polarized basis sets as well as two solvation models, namely COSMO[23] and its extended version IEF-PCM,[17] were used in these supplementary computational efforts. As a result, a little more uniform conformational landscape of the molecules **1a**–**c** emerged from these new higher-quality predictions. Simultaneously, an accuracy of three contemporary NMR-focused protocols (δ_C, δ_H, and $^nJ_{HH}$) was estimated for the case of multiple systems under this study. On the other hand, satisfying reliability of both applied chemical shift-based approaches was confirmed (especially for **1a**) by a recently introduced DP4 'probability' analysis.[12e]

The above findings, being in line with a few recent scarce reports on some molecular parameters (e.g., microwave[24] or circular dichroism[25] data) of the other flexible systems, indicate a need for large caution in drawing up conclusions on overall shapes, energetic and spectroscopic properties of the molecules capable of existing in more than two easily accessible conformers. Evidently, in these circumstances an agreement between theory and observation strongly depends on the reliability of the predictions, and so accurate QM calculations at the TZ-quality level are needed.

As for NMR parameters, a preferential use of high-level δ_H-based protocols involving simulations of the surrounding medium is recommended. Moreover, an analogous control application of the J_{HH} data is strongly proposed in all possible cases. To the best of our knowledge, this is the first parallel application of the δ_C, δ_H, δ_K-DP4, and J_{HH}-based approach versus vdW-DFT corrected energetics

(treated as certain kind of the 'reference data') to the remarkably averaged NMR quantities measured in solutions, for assessing the conformational distributions of flexible molecules possessing several low-energy forms. Some pitfalls in the translation of such an experimental NMR response in structural terms and conformer populations η_Xs were highlighted here, and our approach to solve them might have general relevance.

2. Results and discussion

2.1. NMR signal assignments and standard energy data for the forms A–C of molecules 1

Selected fully assigned ^{1}H NMR chemical shifts, δ_Hs, as well as related geminal and strongly averaged vicinal interproton couplings ($^2J_{HH}$ and $^3J_{HH}$, respectively) found for *N*-methyl pyrrolidin-2-(thi)ones **1** in solution are summarized in Table 1. These spectroscopic molecular data were explained as coming from rapid equilibria between the members of suitable lowest energy conformational families of 1,4-disubstituted heterocycles **1** with the group R in the ring C-4 position diversely oriented in space. Indeed, three distinct forms **A**–**C** of the molecules of **1a**–**c** were always B3LYP/6-31G(*d*)-localized as stationary points on pertinent gas-phase[16] Born–Oppenheimer potential energy surfaces (PESs). Zero-point energies (ZPEs) favor forms **B** and, consequently, differences in relative energies of their conformational isomers are small. Hence, the maximum values were ΔH_0=5.1 kJ mol^{-1} and, especially, $\Delta G^{\circ}_{298.15}$ = 3.6 kJ mol^{-1} as estimated for the form **B** of **1b** (hereafter referred to as **1bB**); see Table 2, numbers in boldface type. This made any determination of relative conformer populations η_Cs of the systems **1a**–**c** in solution based purely on such inaccurate energy predictions practically unreliable.[4b,d,i]

The conformational forms **A**–**C** adopt envelope-type shapes of the five-membered (thio)lactam-ring moiety with an exocyclic substituent R placed in the most puckered segment of the heterocycle. This functional group is disposed pseudoequatorially in the form **A** (lowest-energy global minima) and their rotamers **B**, whereas it is oriented pseudoaxially in isomers **C** (Fig. 1). As for

Table 1
^{1}H NMR data for pyrrolidin-2-(thi)ones **1a**–**c** recorded in $CDCl_3$ at 200 MHz, ppm or Hz[a]

Comp	H-3c	H-3t	H-4	H-5c	H-5t	Other groups
1a[b]	2.82dd[c]	2.54dd[c]	3.57mc	3.75dd	3.40dd	Me 2.91 pt[d]
	$^2J_{3,3}$=(−) 16.8			$^2J_{5,5}$=(−) 9.1		Ph[e]
	$^3J_{3,4}$=8.9	$^3J_{3,4}$=8.0	Σ^3J=31.6	$^3J_{4,5}$=8.0	$^3J_{4,5}$=6.7	
1b	3.46dd[c]	3.14dd[c]	3.63mc	4.10dd	3.76dd	Me 3.31 s
	$^2J_{3,3}$=(−) 17.4$_5$			$^2J_{5,5}$=(−) 11.0$_5$		Ph 7.16–7.39m
	$^3J_{3,4}$=8.4	$^3J_{3,4}$=7.1	Σ^3J=30.4	$^3J_{4,5}$=8.1	$^3J_{4,5}$=6.8	
1b[f]	3.32$_5$dd	2.97dd	3.68mc	4.19dd	3.82dd	Me 3.25 s
	$^2J_{3,3}$=(−) 17.3			$^2J_{5,5}$=(−) 11.0		Ph 7.20–7.39m
	$^3J_{3,4}$=8.5	$^3J_{3,4}$=7.5$_5$	Σ^3J=30.6$_5$	$^3J_{4,5}$=8.0	$^3J_{4,5}$=6.6	
1c	2.77 br s[c]		4.16mc	3.63dd	3.78dd	Me 2.89pt[d]
	$^2J_{3,3}$ not observed[g]			$^2J_{5,5}$=(−) 9.9		Ph[h]
	$^3J_{3,4}\cong$(−) 8.7	$^3J_{3,4}\cong$(−) 8.7	Σ^3J=32.3	$^3J_{4,5}$=9.0	$^3J_{4,5}$=5.9	

[a] Indexes **c** and **t** mean the cis and trans orientation in relation to H-4.
[b] Good agreement with the numerical data reported by Sato et al.[26] was found.
[c] An additional, small (J ~0.7 Hz) long-range coupling with the *N*-Me group protons was observed (see text).
[d] The small coupling with 3-CH_2 protons was observed.
[e] See Table 5.
[f] In $(CD_3)_2CO$ solution.
[g] Not found due to a virtual chemical shift equivalence of both H-3 nuclei.
[h] See Experimental.

Table 2
Important geometric, energetic, and first vibrational mode data for the favored conformers **A**–**C** of molecules **1a**–**c** as in vacuo computed by B3LYP/6-31G(*d*) method

Comp	Form	Torsion angle θ,[a] deg	Classical energy, E_{el},[b,c] Ha	Relative ΔE_{el}, kJ mol^{-1}	Scaled *ZPE*,[c,d] Ha	Relative ΔH_0,[e] kJ mol^{-1}	Relative ΔG°_{298}, kJ mol^{-1}	Population η_C, %[f]	First harmonic vibrational mode,[g] ω_1, cm^{-1}
1a	**A**	−58.3	−556.994 804	0	0.214 145	0	0[h]	55.2	40.9
	B	19.6	−556.992 954	4.86	0.214 075	4.67	2.92	17.0	14.9
	C	−61.6	−556.993 617	3.12	0.214 157	3.15	1.70	27.8	23.1
1a[i]	**A**	−58.3	−557.013 599	0	0.213 562	0	0[h]	53.7	40.8
	B	19.5	−557.011 804	4.71	0.213 492	4.53	2.70	18.0	14.4
	C	−62.2	−557.012 414	3.11	0.213 560	3.10	1.59	28.3	22.6
1b	**A**	−58.4	−879.952 679	0	0.211 973	0	0[h]	57.5	39.5
	B	23.1	−879.950 669	5.28	0.211 896	**5.08**[j]	**3.62**[j]	13.4	16.3
	C	−43.9	−879.951 505	3.08	0.211 984	3.11	1.68	29.2	20.1
1c	**A**	98.0	−670.324 135	0	0.223 857	0	0[h]	54.8	27.0
	B	19.5	−670.323 281	2.24	0.223 763	2.00	1.85	26.0	23.5
	C	106.0	−670.323 094	2.73	0.223 891	2.82	2.59	19.3	27.3

[a] The C3–C4–C_{ipso}–C_{ortho} or C3–C4–C=O exocyclic torsional angle characterizing the fully relaxed structure; its clockwise direction is considered as positive.
[b] A classical (raw) total electronic energy E_{el} for a hypothetical, non-vibrating species.
[c] In hartrees, the atomic units of energy (1 Ha=2625.500 kJ mol^{-1}=627.5095 kcal mol^{-1}=219474.6 cm^{-1}).[27]
[d] The 0.97-scaled[28] raw zero-point energy (*ZPE*) correction was used.
[e] An enthalpy at T=0 K (corrected for *ZPE*), $H_0=E_{el}+ZPE$.[27]
[f] Apparent values given only for a purpose of comparison with other computational results of this work (see also Table 7).
[g] The lowest harmonic vibrational frequency characterizing the located stationary points.
[h] The predicted absolute value of ΔG^0_{298} is of −556.819240, −556.838623,[i] −879.780387, and −670.141176 Ha for **1a**, **1a**,[i] **1b**, and **1c**, respectively.
[i] The B3LYP/6-31G(*d*,*p*) results.
[j] The greatest values discussed in the text.

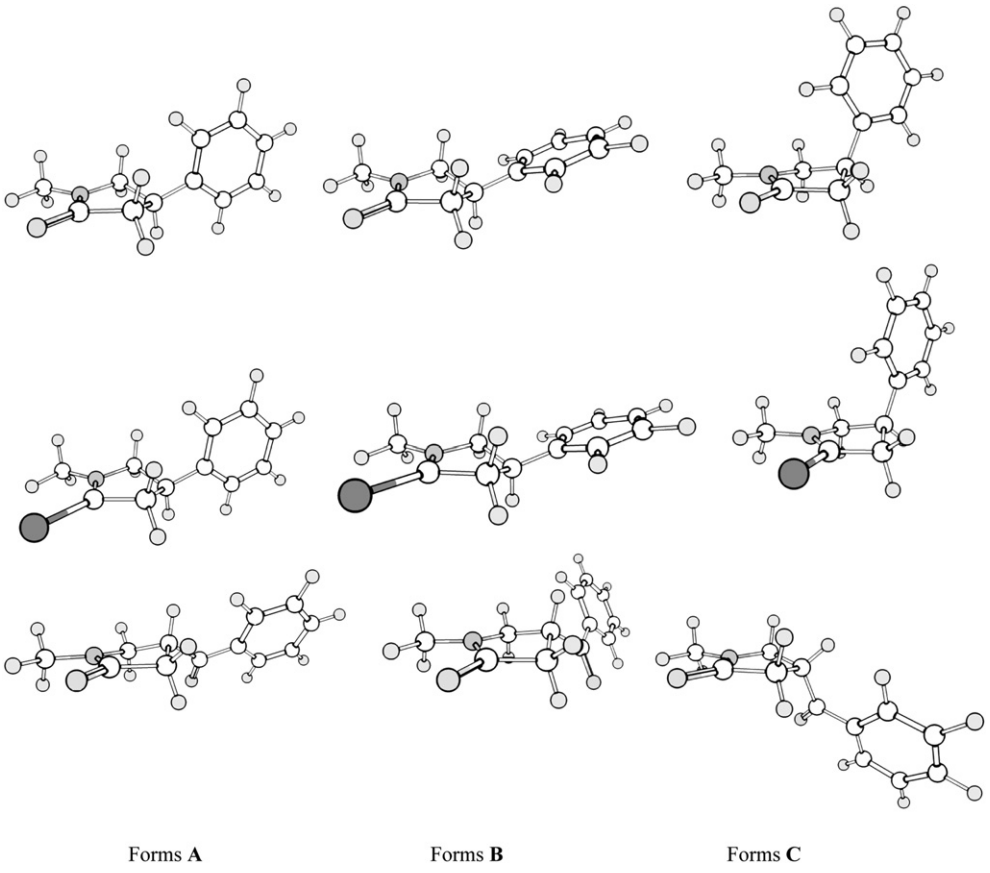

Fig. 1. 3D ChemCraft[29] drawings of in vacuo B3LYP/6-31G(*d*)-located geometries of low-energy equilibrating forms **A**–**C** of the (4*R*)-enantiomers of pyrrolidin-2-(thi)ones **1a** (top), **1b** (middle) and **1c** (bottom).

isostructural molecules **1a** and **1b**, the phenyl (Ph) group is placed almost perpendicularly to their average hetero-ring plane and lies approximately in this plane, respectively, in two rotamers **A** and **B**. Accordingly, the scheme of mutual low-energy interconversions between forms **A**–**C** can be proposed for all investigated entities **1a**–**c** (Fig. 2). Indeed, their PESs are likely to be rather flat, so these systems will spend a lot of time between the conformers mentioned above. Hence, the superposition of pertinent equilibrating forms **A**–**C** leads to the overall conformations of the systems **1** in solution. The only question open was a relative participation (fractional populations, ηs) of these distinct conformers in the ensemble of all possible forms.

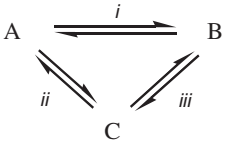

Fig. 2. The proposed scheme of rapid conformational equilibria of the key forms **A**–**C** of systems **1a**–**c**; *i*=rotation, *ii*=5-membered ring pseudorotation, *iii*=both of the motions *i* and *ii* occurring together.

Initially, four independent methods of contemporary calculational chemistry were parallelly applied for a deeper understanding the measured NMR data, i.e., two common approaches based on the chemical shifts (δ_C or δ_H) and two protocols in which intra-ring J_{HH}-couplings were considered instead; see Computational details. A linear regression analysis of the NMR parameters for solution against related gas- or solution-phase B3LYP predictions was followed by empirical scaling[2b,3,4a,c,e,h–j,10,12e,15c–e,18] the results achieved in this way (especially, those concerning the δ_Ks, vide infra). All distinct conformers **A**–**C** of the molecules **1a**–**c** were always included in the analysis.

We begin our discussion with the NMR spectra of **1a** and **1b**. The latter thiolactam system was studied in chloroform ($CDCl_3$) and acetone [$(CD_3)_2CO$]. Its spectroscopic data measured in these two solutions were generally comparable; see Table 1 and Experimental (^{13}C NMR data). An application of acetone resulted in much better separation of the lactam ^1H signals of **1b** at the frequency of 200 MHz. Thus, its H-4 and H-5 resonances are slightly deshielded, while both H-3 multiplets are substantially shielded in this medium. Undoubtedly, these NMR effects mainly result from specific solvent-solute interactions involving the exocyclic functional group C=Y (where Y=O or S). But, the solvent change had only a minimal influence on the diagnostic three-bond $^3J_{H-C-C-H}$ couplings, as expected.[30] On the other hand, a long-range coupling constant ($^5J_{HH}=0.7_3\pm0.0_5$ Hz) between both ring protons in the C-3 position and *N*-Me group protons of **1b** measured in $CDCl_3$ was not observed in $(CD_3)_2CO$, even under the used resolution enhancement[31] conditions (Table 1). Interestingly, similar coupling ($J=0.6_7\pm0.1$ Hz) between *N*-Me protons and one ring proton in the C-4 or C-5 position, was found many years ago for the single bicyclic photoproduct **4a** in CCl_4.[32] Such coupling was not observed for its stereoisomer **4b**. We will return to NMR data for these two rigid lactams **4** again.

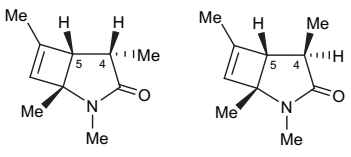

4a **4b**

2.2. Assigning the preferred forms of 1a–c by GIAO NMR calculations (η_Cs, η_Hs)

Let us consider in detail our results from the standard DFT GIAO-based approach found using the δ_Cs alone. The first question concerns the matter of taking into account such NMR data concerning the functional groups C=Y mentioned above. This is a more general topic[33] (so-called *electron correlation* issue)[33d] related to the reliability of molecular properties calculationally predictable at different levels of electronic-structure theory. Especially, it is related to systems presenting an extensive electron conjugation and/or a lot of highly polarizable lone pairs,[10] i.e., $-I^-$ substituents.[33a] The above description indicates that this problem really concerns entities in which operate considerable *dispersion interactions* discovered and formalized by London (vide supra).

The GIAO results for **1a** and **1b** suggested the need for omitting such molecular fragments in a linear regression analysis of calculated versus experimental ^{13}C NMR data. Indeed, their exclusion makes for considerably higher values of the Pearson correlation coefficients r or factors r^2 for both these compounds. Analogous conclusions about the removal of some DZ-quality predicted δ_Cs for low-field carbon atoms, such as sp^2-type nuclei resonating in the 130–220 ppm range, were also drawn by others authors.[34] Two different linear trends found for two regions of the ^{13}C NMR spectrum, which was attributed to *electron correlation effects*,[10] led even to a recent suggestion of the multi-standard approach for GIAO ^{13}C NMR calculations.[35] Our proposition of exclusion of the discussed $\delta_{C=Y}$ data was also in agreement with a recent notion that differences between the δ_Cs of carbon atoms of similar types should be calculated more accurately than the chemical shifts themselves, due to error cancellation.[3b,c,4i,12c,36] In fact, systematic errors in the δ_Cs GIAO-predicted at different levels of approximation were many times empirically corrected in the literature.[37] Accordingly, δ_Cs for the groups C=Y (where Y=O, S) were omitted in all our subsequent calculations.

It should be noted at this point, that computed data Z^{calcd} were always plotted against experimental data Z^{obsd}, and the least-squares linear fitting values of the slope a and intercept b as well as correlation factors (r or r^2) were individually found in this way. Computed Z^{calcd}s were corrected next, by using so-obtained regression parameters a and b, affording the new sets of scaled NMR data (Z^{scaled}s).[2b,3,4e,h–j,10,12e,15d,e,18,38] Indeed, all NMR-focused protocols were followed here by a two-step[2b,3,4i] empirical scaling of the initial correlations of calculated versus experimental data; cf., Fig. 3. It is generally assumed that such a scaling of the predicted NMR parameters by means of the linear regression analysis partially or even completely[4i] compensates systematic errors (associated with the smaller basis sets, inaccurate density functionals, and gas-phase approximation usually used in a vast majority of current computational strategies) and so takes solvent effects into account to some degree.[2b,3,4i,15a,18] The latter effects are usually accepted as being especially influencing the δ_Hs (vide infra).

The next and much more serious issue concerns an apparent absence (or only minor presence) of the forms **A**, reflecting the vacuum global energy minima in conformer ensembles of molecules **1a**–**c** in solution. Thus, **A**:**B**:**C** ratios of ~3:81:16 (r^2=0.9994) and ~0:90:10 (r^2=0.9995) were concluded for **1a** and **1b**, respectively, from standard analysis of the relation $<\delta_C^{calcd}>$ versus $<\delta_C>^{obsd}$, where the notation $<Z>$ means an NMR parameter Z (δ_K or J_{KL}) Boltzmann-weighted averaged for all possible forms (Table 3). In fact, the averaged predicted spectra always displayed some improvement over those of the individual conformers (vide infra). An exemplary plot of this (deceptively good, as it turned out later) relation for **1b** is shown in Fig. 3a. However, such a strong conformational preference for **1bB** over **1bC** and the total absence of **1bA** were in great discord with the related in vacuo energy data ΔH_0 and, especially $\Delta G^\circ_{298.15}$ (cf., Table 2). Moreover, considerably different results were obtained in the second $<\delta_C^{calcd}>$ versus $<\delta_C>^{obsd}$ approach. Indeed, **A**:**B**:**C** ratios of ~20:49:31 (r^2=0.9991) and ~12:60:28 (r^2=0.9992, Fig. 3b) were found for **1a** and **1b** in this manner, respectively (Table 3). All four relevant statistical indicators are given in related plots, namely, two correlation coefficients (r and its square r^2), standard deviation (SD), and the corrected mean absolute error [CMAE,[12c] defined as $(\Sigma_i|Z^{scaled}-Z^{obsd}|)$/number of comparisons ($i$)] as two estimates of the uncertainties of results.

As for relations $<\delta_K^{scaled}>=(<\delta_K>^{calcd}-b)/a$ shown in Fig. 3 (derived from least-squares lines of the form $<\delta_K^{calcd}>=a\times<\delta_K>^{obsd}+b$), it should be noted that the pertinent magnitude of the slope a evaluated for the ^{1}H data was a lot closer to the ideal value of unity than the analogous magnitude estimated for related ^{13}C data. The values of SD and CMAE were also found to be very small in the former case. These findings suggested a high trustworthiness of the δ_H-based conclusion. But, such results are usually considered as less reliable data, i.e., leading to smaller values of r^2; this regularity was also confirmed here. In fact, protons are located

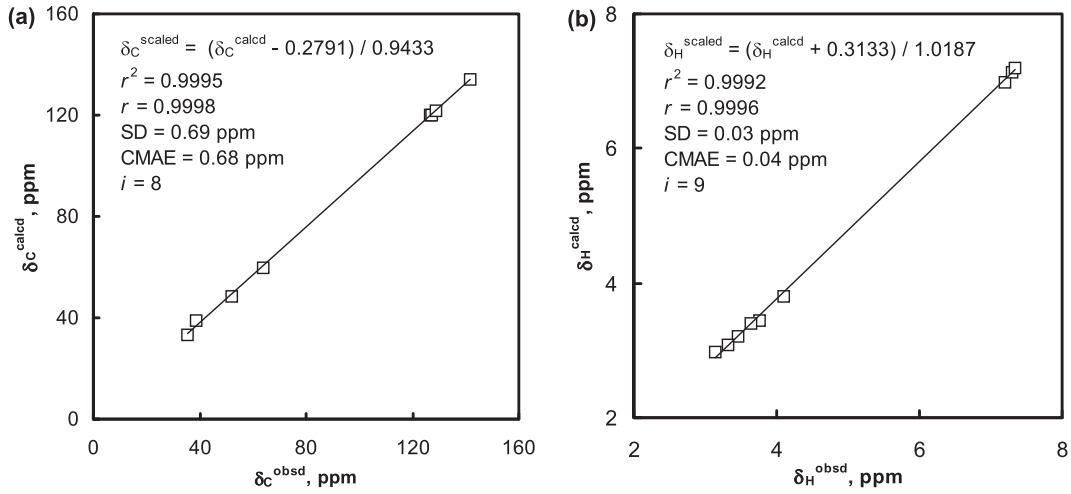

Fig. 3. Deceptively good scatter plots of the calculated versus experimental δ_Ks found for B3LYP/6-31G(d)-level overall multi-component equilibrium conformation of **1b** (gas-phase approximation); a (left side): DZ-level δ_C data, **A**:**B**:**C** ~0:90:10. b (right side): DZ-level δ_H data, **A**:**B**:**C** ~12:60:28.

Table 3
The composition (%) of conformational mixtures of systems **1** in solution found for their DZ-level structures using three DFT methods and the DP4 approach[12e]

	Method	r^2	SD[a]	CMAE[a]	**A**:**B**:**C**
1a	δ_C	0.99939	0.80	0.86	3:81:16
	δ_C[b]	0.99904	0.97	1.10	0:91:9
	δ_C[c,d]	0.99943	0.70	0.89	7:93:0
	δ_C-DP4[c,d]				5:95:0
	δ_H	0.99912	0.04	0.04	20:49:31
	δ_H[b]	0.99893	0.05	0.04	24:57:19
	δ_H[c–e]	**0.99976**	**0.02**	**0.02**	**35:18:47**
	δ_H-DP4[c–e]				34:8:58
	J_{HH}[f]	0.99946	[0.16]	[0.14]	69.5:0:30.5
	J_{HH}[d,f]	0.99887	[0.23]	[0.20]	69.5:0:30.5
	J_{HH}[d,g]	0.99973	[0.09]	[0.11]	66.5:0:33.5
1b	δ_C[h]	0.99951	0.69	0.68	0:90:10
	δ_C[d]	0.99982	0.39	0.44	0:91:9
	δ_C-DP4[d]				2:98:0
	δ_C[i]	0.99992	0.17	0.36	2:81:17
	δ_C[c,d]	0.99949	0.70	0.70	8:78:14
	δ_H	0.99922	0.03	0.04	12:60:28
	δ_H[d]	**0.99964**	**0.02**	**0.03**	**29:30:41**
	δ_H-DP4[d]				44:29:27
	δ_H[i]	0.99728	0.05	0.08	36:26:38
	δ_H[c,d]	0.99880	0.04	0.05	36:25:39
	J_{HH}[f]	0.99951	[0.12]	[0.21]	66:0:34
	J_{HH}[d,f]	0.99981	[0.09]	[0.10]	67:0:33
	J_{HH}[d,g]	0.99956	[0.10]	[0.17]	64.5:0:35.5
	J_{HH}[f,i]	0.99983	[0.04]	[0.13]	47:21:32
	J_{HH}[g,h]	0.99980	[0.03]	[0.15]	29:36:35
1c	δ_C	0.99969	0.57	0.84	0:35:65
	δ_C[c,d]	0.99963	0.74	0.83	20.5:79.5:0
	δ_C-DP4[c,d]				2.5:95:2.5
	δ_H	0.99514[j]	0.06[k]	0.14[k]	14:43:43
	δ_H[c,d]	0.99937[j]	0.03[k]	0.04[k]	0:36.4:63.6
	δ_H-DP4[c,d]				20:0:80
	J_{HH}[f]	0.99158[j]	[0.29][k]	[0.52][k]	19:56:25
	J_{HH}[d,f]	0.99219[j]	[0.35][k]	[0.46][k]	27:51:22
	J_{HH}[d,g]	0.99005[j]	[0.28][k]	[0.58][k]	24:51:25

[a] In ppm or [Hz].
[b] The B3LYP/6-31G(*d*,*p*)//B3LYP/6-31G(*d*,*p*) results.
[c] Functionals[15e] WC04 or WP04 applied at the TZ level.
[d] IEF-PCM/$CHCl_3$.
[e] See Table 5.
[f] IGLO-II used.
[g] IGLO-III used.
[h] See Fig. 3.
[i] IEF-PCM/$(CH_3)_2CO$.
[j] The low value most likely due to strong degeneration of the ^1H and *J* data.
[k] The high value most likely due to strong degeneration of the ^1H and *J* data.

outside organic entities and, therefore, they are subject to more efficient intermolecular solvent-solute interactions than the internally situated carbon atoms of their backbones.[4h,18b,c,e,36,38]

In order to account (at least in part) for the influence of solution-phase environments, two additional standard IEF-PCM[17] simulations of solutions in chloroform and acetone were performed for **1b**, which was examined in these two deuterated solvents. The greatest geometry change was computed for the conformer **1bC**, in which the torsion angle θ (for its definition, see Table 2) increased from −43.9° (vacuum) via −50.7° ($CHCl_3$) to −52.0° [$(CH_3)_2CO$]. Final distribution of its conformer **C**, η_C(**1bC**), in the first solution, estimated from such PCM/$CHCl_3$-based δ_Cs, was almost identical with the in vacuo population ratio (**A**:**B**:**C** ~0:91:9, r^2=0.9998; Table 3). In contrast, the parallel computed δ_Hs provided the otherwise conformational picture of **1b** in $CDCl_3$ (**A**:**B**:**C** ~29:30:41, r^2=0.9996), with a greater molar fraction of the form **A**, η_H(**1bA**) ~ 0.29. Instead, a growth in participation of **A** at the expense of **B** or **C** was found through the δ_Cs- and, especially, δ_Hs-based approaches, by considering results from related PCM simulation of **1b** 'dissolved' in more polar $(CH_3)_2CO$. Again, the larger contribution of **A** in the conformer mixture was inferred from the δ_Hs, η_H(**1bA**) ~0.36. On the other hand, these mutually inconsistent δ_Cs versus δ_Hs results obtained from IEF-PCM solvation studies were in agreement with the aforementioned generalization[4h,18b,c,e,36,38] on the solution-phase environment 'resistant' δ_Cs versus medium 'susceptible' δ_Hs.

Moreover, to check the reliability of our methodology of NMR computations for the lactam systems, similar calculations of δ_Hs were also performed for both isomers of the rigid bicycle **4** (vide supra). The gas-phase GIAO B3LYP/6-31G(*d*) predictions, obtained for the ratio **4a**/**4b**=1:1, reproduced the reported data[32] reasonably well (r^2=0.9972, SD=0.05 ppm, CMAE=0.06 ppm, *n*=14). Analogous TZ-level B3LYP/6-311+G(2*d*,*p*)//B3LYP/6-31G(*d*) runs performed with the IEF-PCM/CCl_4 simulation of solvation gave the considerably better result (r^2=0.9992, SD=0.03 ppm, CMAE=0.04 ppm, *n*=14). These not very high values of r^2 were explainable by a low accuracy of the early 60-MHz ^1H NMR data, due to the overlapping multiplets.

Simultaneous consideration of the foregoing 'individual' gas-phase δ_C and δ_H results for **1a** and **1b** led to average (and, most probably, more realistic)[12c,e] **A**:**B**:**C** ratios of ~11:66:23 and ~6:75:19 for their three-component conformer mixtures, respectively. Therefore, an estimated uncertainty of their GIAO-derived NMR data was in the order of 15%. However, the true presence of forms **A** should be assumed, especially for **1a**. The latter conclusion was in line with δ_H-based results from PCM simulations done for **1b** in two explicit solvents and, especially, with the chemical intuition. Similar uncertainty (10–15%) of the GIAO-supported evaluations of the composition of multi-conformer mixtures in aqueous solution was found recently.[3b] In view of all these findings, the above NMR-based results on **1a** and **1b**, with the only minor participation of their forms **A**, seemed trustworthy and mutually consistent.

Indeed, certain conformers allocated as global energy minima in the gas-phase were sometimes not recognized in solution, by using in vacuo GIAO-supported analysis of the experimental NMR data.[3] Generally, discrepancies of this kind are explained by specific solvent–solute effects and, especially, molecular motions only seldom adequately considered (if at all) in a predominant majority of computational treatments in normal use.[3,4a,i,15a,18] In fact, for typical liquid-phase samples at room temperature, many vibrational levels are populated, in particular low-frequency vibrations, and the measured NMR quantities are actually thermal averages over the zero-point motion and over a Boltzmann distribution of thermally accessible vibrational states.[39] Accordingly, it was postulated that for some multi-conformer systems the '*solution-phase environment (spectroscopic) match criterion*', i.e., the best root-mean-square fitting to the solution NMR data, is the stronger determinant for a structural goodness of their key contributing forms than standard '*energetic criterion*'.[3,40] Similar conclusions were drawn also by other authors.[4b,d,i] Hence, the usually recommended[2b,4e–h,j,12,15e,18d,e,34c] evaluation of population-averaged NMR parameters, calculated taking into account Boltzmann-population-weighted contributions of each low-energy conformer to total equilibrium population evaluated from related energy data (ΔE_{el}, ΔH_0 or, much better, ΔG°) computed in normal manner, were not applicable for such molecules. The two highly flexible systems **1a** and **1b** reflected this case very well.

At a first sight, very comparable results were also found for the last oxo compound **1c**. Likewise, an exclusion of δ_Cs of its lactam group C=O makes for a better correlation. Thus, the **A**:**B**:**C** ratio of ~0:35:65 was assessed from such a reduced δ_Cs set (r^2=0.9997). Again, the substantial contribution of **A** was only obtained applying the δ_Hs. All three conformers of **1c** were recognized in this way, **A**:**B**:**C** ~ 14:43:43 (r^2=0.9951; Table 3). Fortunately, both geminal protons in the C-3 position of **1c** were found as virtually chemically equivalent under the used NMR measurement conditions ($\Delta\delta_H \cong 0$ ppm, Table 1), in sharp contrast to analogous nuclei in **1a** and **1b**. This fact complicated the whole analysis, however it was also very helpful. Indeed, the shift difference in δ_Hs predicted for

these two protons in **1c** was found to be 0.23, 1.33, and 0.60 ppm for its form **A**, **B**, and **C**, respectively. Such $\Delta\delta_H$s strongly suggested the participation of **1cA** in conformer ensemble at the expense of **1cB**. This finding was in qualitative agreement with the above conclusion based on δ_Hs, but in strong opposition to the parallel result inferred from the δ_C data alone.

2.3. The population of the forms A–C of lactams 1a–c through J_{HH} data (η_Js)

In an attempt to explain the aforementioned conflicting results, a third *J*-approach was used, relying on interproton couplings in the flexible systems **1a**–**c**. It was shown previously[2b] that GIAO-predicted δ_Hs (despite high values of r^2 provided by a linear regression analysis) are, generally, not as good as probes for approximating the intramolecular motions as proton–proton coupling constants, J_{HH}s. Indeed, J_{KL}-couplings are generally not significantly influenced by the solvent, e.g., by formation of external hydrogen bonds, and thus can be considered dependent predominantly on molecular structure and conformation.[4d] The necessary supporting use of *J* data for the case of small equilibrating molecule was also employed by Cimino et al.[4f]

Accordingly, two different theory levels for predicting J_{HH}s were used here for the multi-conformer systems **1**. The first was an advanced DFT B3LYP/IGLO-II//B3LYP/6-31G(*d*) method[41] embracing the calculation of all internucleus $^nJ_{KL}$ data together, by using an NMR-oriented IGLO-II[22] basis set comparable to other basis sets of triple-ζ valence quality with polarization functions[22b] (for a graphical illustration of the results see Fig. 4a). In the second approach, the Haasnoot et al.[42] empirical modification of the Karplus equation was used, which supplies the vicinal $^3J_{HH}$s only. The J_{HH} values computed at these two levels of approximation are gathered in Table 4; the gas-phase B3LYP/6-31G(*d*)-optimized structures of all nine low-energy structures **A**–**C** of **1a**–**c** were considered.

best-fit line, $^3J_{Karplus}$ [Hz]=0.8867 $^3J_{DFT}$+0.9184 (Fig. 4b), evaluated for 36 pairs of $^3J_{HH}$s given in Table 4. Moreover, very helpful $^nJ_{HH}$s ($n\neq3$) are not predictable by the Karplus-type relationship.

The $^nJ_{HH}$-based conformer populations, η_Js, found for **1a**–**c** applying the gas-phase DFT approach mentioned above, are also presented in Table 3. Thus, ~2:1 ratio of forms **A** and **C** and the total absence of **B** were estimated for both isostructural systems **1a** and **1b** (Fig. 4a). In every case, the eight $<^nJ_{HH}s>$ couplings were applied, i.e., two ^2J, four ^3J, and two ^5J data points. Such a good agreement on $^nJ_{HH}$ data sets was not found with **1c**, for which a large contribution of **B** at the expense of **A** and **C** was estimated; the **A**:**B**:**C** ratio of ~19:56:25. However, a weaker correlation established in this case should be noted (r^2 of 0.9916 and, especially, CMAE=0.53 Hz). Undoubtedly, this effect was resulted (at least in part) from the substantial degeneration of the experimental *J*s data for **1c** (one ^2J, two ^3J, one $^3J_{av}$, and two ^5Js). Therefore, it was rather difficult to draw out any definitive J_{HH}-based result on the conformer ensemble in solution for this molecule, at this stage.

In reality, the above calculations of η_Js based on J_{HH}-couplings in systems **1**, complicated the whole situation instead of explaining it. Especially spectacular was the case of **1b** where contributions of its equatorial forms **A** and **B** in an equilibrium mixture were quite variously assessed, depending on the method used. Thus, the **A**:**B** ratio of 0:90, 12:60, and 66:0 was deduced according to the δ_C, δ_H, and $^nJ_{HH}$ NMR data, respectively (Table 3, Figs. 3 and 4a).

Consequently, the DFT B3LYP/IGLO-II//B3LYP/6-31G(*d*) approach was also applied for two rigid isomeric systems **4**,[32] as test lactams. Two variants were employed, i.e., for the gas-phase state and solution in CCl_4 (the later simulated via an IEF-PCM technique). In both cases, a small long-range coupling $^5J_{HH}$=0.6$_7$±0.1 Hz was reproduced only for lactam **4a**, in agreement with the literature; J^{calcd} of 0.72 Hz (gas) or 0.78 Hz (CCl_4). Simultaneously, this spin–spin interaction was unambiguously found as occurring between *N*-Me group protons and ring protons in the C-4 position.

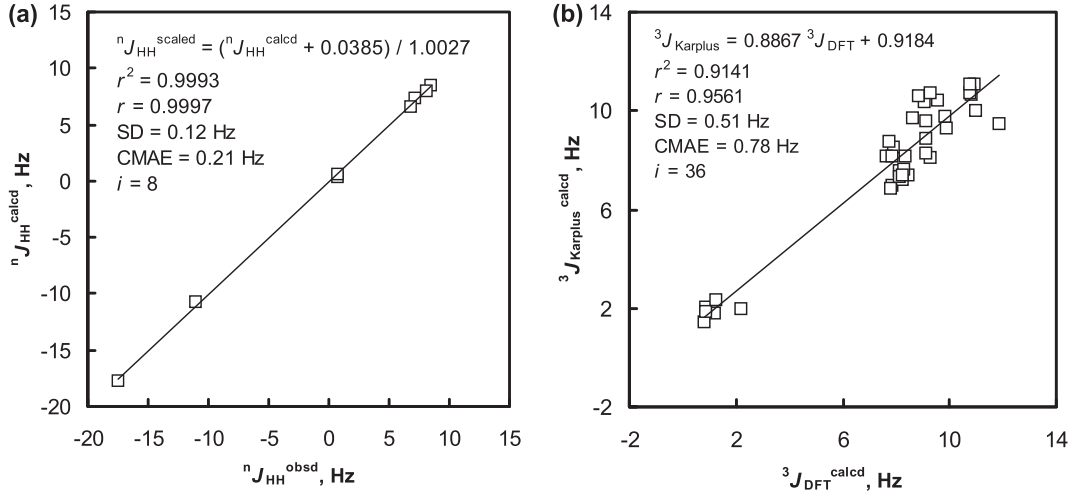

Fig. 4. Scatter plots of various $^nJ_{HH}$s for the B3LYP/6-31G(*d*) structures (a, left side): the two-component overall conformation of **1b** (**A**:**B**:**C** ~66:0:34) wrongly estimated initially, by using the eight pairs of $<^nJ_{HH}s>$ data; see text. (b, right side): the relation $^3J_{Karplus}$ versus $^3J_{DFT}$ evaluated for 36 pairs of the $^3J_{HH}$ data points collected in Table 4.

Inspection of the content reveals that ^3J data estimated with the modified Karplus equation[42] should be discarded. This simple and very fast method, thought useful enough in an initial qualitative analysis of ^{1}H NMR spectra, is less sensitive to structural changes in the molecules. Indeed, some values of $^3J_{HH}$ were quite differently calculated, especially for $^3J_{4,5u}$ data (Table 4, data highlighted in bold type). Similar differences between the J_{HH} data sets estimated in this way and their real values measured experimentally were reported previously.[39,43] Thus, moderately good values of r^2=0.9141, but rather large SDs and CMAEs were found for the Karplus relation

The second *J*-data reported for **4a**, $^3J_{4,5}$=9.8±0.5 Hz,[32] was also predicted very well; J^{calcd} of 9.57 or 9.65 Hz (gas or CCl_4). Hence, the high reliability of such a computational protocol for predicting the $^nJ_{HH}$s in other structurally similar lactams was shown.

2.4. An analysis of the problem of incompatibility of the η_X results

It was obvious that the foregoing issue with a correspondence between different calculational NMR results on η_Xs for the title

Table 4
The intra-ring J_{HH}s in forms **A**–**C** of **1a**–**c** as calculated by the DFT B3LYP/IGLO-II//B3LYP/6-31G(*d*) method[41] or using the Karplus-type equation[42] (data in parentheses), Hz[a]

Comp	Form	$^2J_{3d,3u}$	$^3J_{3d,4}$	$^3J_{3u,4}$	$^2J_{5d,5u}$	$^3J_{4,5d}$	$^3J_{4,5u}$
1a	**A**	−16.48 (−)	8.44 (7.39)	10.80 (10.66)	−9.67 (−)	8.11 (7.56)	**9.04** (**10.35**)
	B	−15.38 (−)	7.86 (7.00)	10.95 (11.10)	−8.91 (−)	8.10 (7.31)	**8.83** (**10.63**)
	C	−17.07 (−)	9.89 (9.33)	1.19 (1.83)	−9.74 (−)	7.92 (8.52)	**0.87** (**2.03**)[b]
1b	**A**	−17.57 (−)	8.21 (7.21)	10.75 (10.72)	−10.72 (−)	8.29 (7.62)	9.56 (10.45)
	B	−16.40 (−)	7.76 (6.86)	10.78 (11.11)	−9.95 (−)	8.21 (7.39)	**9.27** (**10.70**)
	C	−18.02 (−)	9.09 (8.91)	0.78 (1.45)	−10.67 (−)	7.61 (8.17)	0.85 (1.88)
1c	**A**	−16.05 (−)	9.27 (8.11)	11.00 (10.04)	−9.88 (−)	7.85 (8.18)	8.60 (9.73)
	B	−16.97 (−)	8.31 (8.19)	9.82 (9.79)	−9.37 (−)	9.11 (8.29)	9.08 (9.59)
	C	−16.77 (−)	**11.86** (**9.45**)[b]	2.16 (1.98)	−9.34 (−)	7.72 (8.77)	1.25 (2.35)

[a] Data showing greatest differences are given in bold type.
[b] The extreme different $^3J_{HH}$s evaluated by two methods, which were used in comparison (see text).

molecules **1a**–**c** may well lie in the difficulty of computing accurate geometries and relative energies of their three key forms **A**–**C** as it does in final predictions of related NMR δ_K and $^nJ_{HH}$ data. In fact, conformations of flexible five-membered rings are overall hard to calculate effectively. On the other hand, the shape and energy of any form is determined to a large extent by the relatively weak intramolecular nonbonded [*van der Waals (vdW) dispersion-type*] interactions and by solvent effects, which are traditionally difficult to simulate by the standard methods. As for NMR parameters, the *J*-couplings are more sensitive to subtle conformation changes than chemical shifts and supposedly less influenced by the solvents.[4d] The latter generalization was compatible with the situation found in this work, at least for **1a** and **1b**. All NMR-oriented strategies applied here for the calculation of δ_Ks are in common use. Indeed, the DFT/6-31G(*d*) (or superior) and DFT/6-31G(*d*,*p*) method, where DFT=B3LYP or MPW91PW91 density functional, were recently recommended for the structure computation and subsequent evaluation of their NMR chemical shifts, respectively.[12d]

To check if the use of a larger basis set would not have a significant influence on the final results, we also predicted NMR shifts of conformers **A**–**C** of **1a** by the B3LYP/6-31G(*d*,*p*) method (Introduction). As can be seen from Table 2, geometries **1aA**–**1aC** depend only marginally on the level of calculations. Moreover, no awaited improvement in the compatibility of subsequent NMR predictions with the observation was so obtained. Only slightly different conformer populations with an unexpected larger preference of the form **B** were found, by using the δ_H- (changes of 4–12%) or δ_C-data sets (3–10%); see Table 3. Therefore, the final conclusion was not altered.

In addition, two other recently proposed hybrid density functionals, i.e., WC04 and WP04,[15e] specially parameterized to predict δ_Cs and δ_Hs in $CDCl_3$ solution were also applied for 'solvated' structures **1aA**–**1cC** in conjunction with an extended 6-311+G(2*d*,*p*) basis set of TZ quality. In this instance, some substantial changes with relation to initial vacuum NMR results were obtained. The computed δ_Hs of 'solvated' forms **A**–**C** of **1a** compared, either individually or collectively (as an adequate least-squares-weighted average) with the recorded solution $<\delta_H>$ data, are given in Table 5. Neither of the contributing forms, if treated separately, gives an acceptable agreement ($r^2 \geq 0.999$)[15a] between the experimental and computed ^1H NMR spectrum. However, if the so-predicted δ_Hs of these conformers were averaged using their

Table 5
Experimental and $<\delta_H^{scaled}>$ data predicted for the forms **A**–**C** of **1a** in $CHCl_3$,[a] their differences, statistics of relations $<\delta_H^{obsd}>$ versus $<\delta_H^{scaled}>$, selected geometric data, energetics and Boltzmann-weighted fractional populations η_G of these conformers[b]

Nucleus	δ_H^{obsd}	**A**		**B**		**C**		**A**:**B**:**C**=**35**:**18**:**47**	
		δ_H^{scaled}	$\lvert\Delta\delta_H\rvert$	δ_H^{scaled}	$\lvert\Delta\delta_H\rvert$	δ_H^{scaled}	$\lvert\Delta\delta_H\rvert$	δ_H^{scaled}	$\lvert\Delta\delta_H\rvert$
H-3c	2.817	2.719	0.10	2.703	0.11	2.965	0.15	2.832	0.01
H-3t	2.538	2.670	0.13	2.658	0.12	2.396	0.14	2.539	0.00
H-4	3.573	3.607	0.03	3.818	0.24	3.503	0.07	3.595	0.02
H-5c	3.750	3.532	0.22	3.822	0.07	3.821	0.07	3.719	0.03
H-5t	3.404	3.452	0.05	3.200	0.20	3.309	0.10	3.340	0.06
H-Me	2.907	2.967	0.06	2.809	0.10	2.996	0.09	2.953	0.05
H-Ph *ortho*	7.224	7.320	0.10	7.162	0.06	7.216	0.01	7.243	0.02
H-Ph *meta*	7.35	7.324	0.03	7.382	0.03	7.371	0.02	7.356	0.01
H-Ph *para*	7.31	7.282	0.03	7.317	0.01	7.296	0.01	7.295	0.02
$\lvert\Delta\delta\rvert_{max}$			0.22		0.24		0.15		0.06
r^2		0.9974		0.9958		0.9980		0.9998[c]	
SD		0.063		0.077		0.052		0.020	
CMAE		0.082		0.106		0.073		0.024	
DP4 result, η_{DP4}[d]		**0.338**		**0.084**		**0.578**			
Torsion angle θ,[e]		−58.4		17.1		−59.5			
Mode ω_1,[e]		41.3		10.4		22.9			
ΔG°_{298}		0[f]		2.24		2.28			
η_G[g]		(0.555)		(0.224)		(0.221)			
$\Delta G^\circ_{298.15}$ + vdW[g,h]		0		(1.64)		(0.44)			
η_G (vdW)[g,h]		0.425		0.219		0.355			

[a] The approach WP04/6-311+G(2*d*,*p*) IEF-PCM ($CHCl_3$,UA0)//B3LYP/6-31G(*d*) IEF-PCM ($CHCl_3$,UA0) used.
[b] All data (except r^2 and η) in ppm, deg, cm^{-1}, and kJ mol^{-1}, respectively.
[c] The least-squares fit equation: δ_H^{scaled} [ppm]=(δ_H^{calcd}+0.2891)/1.063.
[d] By using the δ_Hs only.
[e] See Table 2.
[f] The 0.97-scaled[28] absolute value of G^0_{298} is equal to −556.829510 Ha.
[g] Apparent data given only for comparison with other results of this work.
[h] With the added DFT-D3[44] total energy corrections for vdW dispersion-type (London) interactions[44,45] estimated with ORCA[46] for B3LYP/G at 0 K (see below in the text and Tables S1–S3).

relative molar fractions ηs determined by the linear regression analysis (i.e., with η_H of 0.35, 0.18 and 0.47, respectively), the resulting spectrum was very close to the one recorded experimentally; r^2=0.9998. In fact, all of these final $<\delta_H^{scaled}>$s were within 0.06 ppm of their experimental counterparts. In contrast, the maximum $|\delta_H^{obsd}-\delta_H^{scaled}|$ value was of 0.22, 0.24, and 0.15 ppm for the single conformers **A**, **B** and **C** of **1a**, respectively.

On the whole, the large participation of forms **A** and **C** in overall conformations of both isostructural systems **1a** and **1b** was deduced in this way for $CHCl_3$ solution from the δ_H data, at the expense of their forms **B** (Table 3). This result was in qualitative agreement with the conclusions based on related *J*-predictions obtained with the use of a fairly large sized IGLO-II basis set (vide supra). Again, substantial changes were found in NMR predictions obtained at the higher level of theory. On the other hand, a greater conformational preference of forms **B** and, especially, **C** at the expense of the conformer **A** was analogously predicted for the oxo lactam **1c**, in large disagreement with an in vacuo energetic order of its forms found at the DZ level (Table 3).

At this time, we realized that above incompatibilities of the η_Xs (where *X* =C, H, *J* or *G*) results for the system **1** could arise in part from too low a level of calculation. Indeed, for flexible molecules only highly reliable methods should be used on every stage. Especially, it is of crucial importance for all considerations on the multi-conformer equilibria involving more than two coexisting forms. It was obvious that any interpretation of the mean values of their experimental NMR data requires the exact knowledge of these quantities for the individual conformers, values that are not available from an experiment. Accordingly, most of our initial NMR calculations on the forms **A**–**C** of **1a**–**c** done within the framework of three series of computational efforts, i.e., options **I** (δ_Cs), **II** (δ_Hs), and **III** (J_{HH}s), were repeated at the triple-ζ (TZ) level with simultaneous modeling $CHCl_3$ solvation; see Table 6. We applied the ORCA suite of programs[46] for this purpose, due to convergence problems with these computations within the Gaussian 03 package.[47] Respectively, two techniques of solvation simulation were employed, namely, COSMO[23] and IEF-PCM[17] as an improved version of the former model, in the first and second stage of these new NMR calculations.

Table 6
Three options used in the second stage of new series **I**–**III** of NMR calculations for the forms **A**–**C** of **1a**–**c** applying their B3LYP(G)/def2-TZVP COSMO ($CHCl_3$) geometries found with ORCA[a]

Option	Subsequent TZ-level NMR computations (using Gaussian)
a	WC04 or WP04/6-311+G(2*d*,*p*) IEF-PCM ($CHCl_3$,UA0)
b	B3LYP/IGLO-II IEF-PCM ($CHCl_3$, UA0)
c	B3LYP/IGLO-III IEF-PCM ($CHCl_3$, UA0)

[a] See also text and Computational details.

Simultaneously, a few of the already used methods were additionally validated.[48,49] Thus, two hybrid density functionals WC04 and WP04[15e] were verified in respect of reliability of the δ_Ks predicted with their use. Instead, two basis sets (IGLO-II and IGLO-III)[22] designed specifically for calculating the magnetic shieldings, σ_Ks, were examined in the goodness of J_{HH} computations. Two training sets of the rigid or conformationally homogeneous molecules were employed, in which the B3LYP/6-31G(*d*) PCM ($CHCl_3$, Bondi's radii)-optimized structures[15e] were used.[48–50] The use of the WP04/6-311+G(2*d*,*p*) PCM/$CHCl_3$ level was really found[49] as a highly reliable method of predicting the δ_Hs, in full agreement with other reports.[15e,h] In sharp contrast, the analogous use of WC04 led to worse results. Regarding two basis sets mentioned above, an extensive IGLO-III basis was the decided winner.[49] Our findings concerning $^nJ_{HH}$-calculations were compatible with the opinion[22c] that IGLO-II, in spite of its good performance, should be applied with some care as it sometimes gives reliable results most likely by a fortuitous cancellation of errors.

2.5. TZ-level η_X results on the molecules 1

Final geometrical and energetic data of nine conformers **A**–**C** of the molecules **1a**–**c** found at the triple-ζ (TZ) level of theory applying ORCA,[47] with the $CHCl_3$ solvation simulated through the COSMO model,[23] are listed in Table 7. [Cartesian coordinates of all these forms are given in Supplementary data (Tables S1–S9).] In general, the new structures were comparable to those predicted initially; cf., Table 2. The greatest difference concerns **1bC** (θ of −50.0 instead of −43.9°), but similar angle θ of −50.7° was already found earlier in standard IEF-PCM ($CHCl_3$, UA0) simulations at the DZ level. On the contrary, there are substantial changes in energetics, especially after an additional energy refinement carried out with the (partially corrected for dispersion energy distribution) double hybrid B2PLYP functional[51] and an additional inclusion of DFT-D3 corrections[44] for intramolecular *London dispersion attraction*.[44,45] (Computational details). These latter terms yielded values for the stabilization energy associated with *vdW dispersion-type interactions*, which were calculated higher for the forms other than global minima (conformers **A**). Consequently, all forms **A**–**C** of the systems **1a**–**c** were recognized as more similar in energy.

Indeed, for some time it has been known that commonly used exchange-correlation functionals do not describe correctly the medium-range *electron correlation* interactions attributed to the *vdW dispersion* (*London*) *forces*.[44,45] So, atom-pairwise specific DFT-D3 corrections[44] to standard DFT energies were evaluated here for the TZ-level structures mentioned above. All these calculations were conducted using ORCA programs.[46] An earlier semi-empirical DFT-D2 approach was inter alia applied in a mechanistic insight into the cyclization reactions of some tryptophan derivatives.[52]

Unfortunately, there was no possibility to perform analytically the thermochemical computations with the ORCA package, while available numerical calculations are too inaccurate,[46] especially[28c] for entities showing very low (but positive) values of the lowest mode frequencies, ω_1s (Table 5). However, as stated above, the differences in geometries of 'solvated' structures **A**–**C** of **1a**–**c** computed at both DZ and TZ levels were rather small. Hence, without committing a greater error, one could roughly estimated the TZ-level Gibbs free energy values of these forms **A**–**C** by addition, to above predicted ΔE_{el}^{corr}s, the 0.97-scaled[28,53] thermal ($G_{298}-E_{el}$) corrections evaluated at the B3LYP/6-31G(*d*) IEF-PCM ($CHCl_3$,UA0) level.

In this way, a reliable semi-quantitative estimation of the fractional conformer populations, η_Gs, based only on energetic data was possible for the lactams **1a**–**c** in $CHCl_3$ as a continuum solvent, for the first time (Table 7). The three major forms of systems **1a** and **1c** were recognized as being rather similarly populated. It was true, in particular, for the latter object **1c**, where forms **A**–**C** were found to be isoenergetic within 0.79 kJ mol^{-1}; ΔG_{298} of 0.00, 0.79, and 0.07 kJ mol^{-1} for **A**, **B**, and **C**, respectively. Since such small relative Gibbs free energies of the local minima (**B** and **C**) are a lot below the Boltzmann quantum (kT ~2.5 kJ mol^{-1}, at the ambient temperature) a semi-free dynamics of these molecules can be deduced.[4d] In sharp contrast, the large predominance of the conformer **C** over **A** and especially **B** was found for the thio system **1b**.

The foregoing η_G data were compared with different NMR-based η predictions of the highest quality, i.e., with maximal values of r^2 (always >0.999).[15a] It was obvious that large values of SDs or CMAEs render any quantitative conclusions on the conformer populations η_Gs unreliable. Inspection of the content reveals that the η_G data for **1a** are in an excellent agreement, 0–4% (i.e., ±2% or better) with the η_{XH} data estimated with the great certainty from δ_Hs (**A**:**B**:**C** ~37:25:38, r^2=0.99995; Table 8). However, for the

Table 7
The key geometrical and energy data for the forms **A**–**C** of molecules **1a**–**c** in $CHCl_3$ solution (modeled by COSMO[23]) as computed by the B3LYP(G)/def2-TZVP method applying the ORCA[46] package[a]

Form		Torsion angle θ,[b] deg	Total energy, E_{el},[c–e] Ha	Relative ΔE_{el},[c,d] kJ mol^{-1}	Refined energy, E_{el},[f] Ha	ΔE_{solv},[g] kJ mol^{-1}	ΔE_{correl},[h] kJ mol^{-1}	Relative ΔE_{el},[f] kJ mol^{-1}	$G_{298}-E_{el}$ correction,[i] Ha	DFT-D3 correction,[j] Ha	Relative vdW term,[j] kJ mol^{-1}	Relative ΔG_{298}^{corr},[k] kJ mol^{-1}	Estimated population η_G, %[l]
1a	**A**	−59.3	−557.217053	0	−556.827050	0[m]	0[n]	0	0.174957	−0.011734	0	0.0	40.9
	B	23.1	−557.215258	4.71	−556.825605	−0.09	−0.10	3.79	0.173858	−0.011880	−0.38	1.18	25.4
	C	−63.9	−557.215492	4.10	−556.826299	0.37	−1.57	1.97	0.174299	−0.012086	−0.92	0.48	33.7
1b	**A**	−59.1	−880.166375	0	−879.719621	0[m]	0[n]	0	0.171710	−0.012519	0	0.0	24.8
	B	23.9	−880.164494	4.94	−879.718082	−0.06	−0.12	4.04	0.171020	−0.012671	−0.40	2.48	9.1
	C	−50.0	−880.164804	4.12	−879.719226	0.96	−1.99	1.04	0.170327	−0.013008	−1.29	−2.43	66.1
1c	**A**	99.8	−670.594871	0	−670.142045	0[m]	0[n]	0	0.181264	−0.013554	0	0.0	37.0
	B	16.0	−670.594382	1.29	−670.141660	−2.06	0.23	1.01	0.181175	−0.013577	−0.06	0.79	26.9
	C	102.5	−670.594298	1.50	−670.142112	−1.41	−0.99	−0.18	0.181277	−0.013731	−0.46	0.07	36.0

[a] See, Computational details.
[b] See Table 2.
[c] The absolute energies from full geometry optimizations at the B3PLYP(G)/def2-TZVP (COSMO) level.
[d] The stabilization by solvation (COSMO model[23]) included.
[e] Total energies after outlying charge correction applied.
[f] Single-point energy refined at the RI-B2PLYP-D[51]/def2-TZVPP def2-TZVPP/C (COSMO) level with the DFT-D3 term included.
[g] The stabilization of the molecular energy by solvation (COSMO/$CHCl_3$).
[h] Relative RI-MP2 correlation energies.
[i] The 0.97-scaled[28] thermal corrections found at the B3LYP/6-31G(*d*) IEF-PCM/$CHCl_3$,UA0 level.
[j] Long-range DFT-D3[44,46b] vdW dispersion (London) corrections to total energy.
[k] The vdW terms included.
[l] Conformer populations, η_Gs, based on ΔG_{298}^{corr}s assessed by addition of DFT-D3 terms to pertinent estimated ΔG_{298}s.
[m] The absolute values are of −0.014555, −0.014859, and −0.018249 Ha for **1a**–**c**, respectively.
[n] The absolute values are of −0.793198, −0.801180, and −0.926894 Ha for **1a**–**c**, respectively.

second system **1b** such an agreement with η_Hs is a little worse, 4–25% (**A**:**B**:**C** ~29:30:41, r^2>0.9996; Table 3) or even 10–29% (**A**:**B**:**C** ~35:28:37, r^2=0.9991; Table 8) but still within ±15%, as expected (vide supra). A predominant participation of **1bC** in its conformational mixture seems to result both from the smallest thermal factor and very large *vdW dispersive attraction* (Table 7). The latter effect manifests itself through most negative values of the ΔE_{correl}s and DFT-D3 terms. Interestingly, these data also correlate fairly well (r^2=0.8990, for six pairs of non-zero values). Most likely, such large *intramolecular London forces* arise from the presence of an easily polarizable group C=S in thiolactam **1b**. Instead, two stabilizing factors, i.e., dispersion and solvation effects, seem to be co-operative in oxo system **1c**, meaning that its conformers **A** and **C** are practically evenly populated.

For the latter oxo lactam **1c**, such conformity between the η_Hs or η_Js versus η_G results is also a little worse, 11–37% or 9–16%, respectively, but all these correlations was found weaker in this case (**A**:**B**:**C** ~0:36:64, CMAE=0.04 ppm or **A**:**B**:**C** ~27.5:51.5:21, CMAE ~0.46 Hz; Tables 3 and 8), especially, the latter J_{HH}-based result is worth noting. On the other hand, δ_Hs and J_{HH}s for **1c** were strongly degenerate and so NMR data-based ηs are less reliable, in general. Interestingly, a significant participation of **1cA** was found only in the J_{HH}-based predictions for $CHCl_3$ solution, η_Js, by applying the IGLO-II or IGLO-III basis set. Almost identical findings were obtained, with the former base, for the DZ- and TZ-level 'solvated' structures of **1c** (9.5–15% agreement, **A**:**B**:**C** ~27.5:51.5:21, CMAE ~0.47 Hz; Tables 3 and 8). Fortunately, three J_{HH}s in its conformers **A** and **B** with an equatorially oriented Ph group differed by 1.1–1.6 Hz and, therefore, differentiation of these forms via a linear regression analysis was possible. Substantial differences in δ_C^{calcd}s among possible contributors to conformational families for the success of regression analysis of the multiple conformer equilibria, was indicated previously by Sebag et al.[4c]

Table 8
Conformer populations of the systems **1a**–**c** in solution estimated at the TZ level through NMR data, %

	Method[a]	r^2	SD[b]	CMAE[b]	**A**:**B**:**C**
1a	Ia[c]	0.99924	0.84	1.00	14.5:85.5:0
	Ia-DP4[c]				11:89:0
	IIa	**0.99995**[d]	**0.01**	**0.01**	**37**:**25**:**38**
	IIa-DP4				32:31:37
	Ia/IIa-DP4				11:89:0
	IIIb	0.99839	[0.27]	[0.24]	21:50:29
	IIIc	0.99933	[0.13]	[0.19]	69:0:31
1b	Ia[c]	0.99913	0.86	0.97	28:72:0
	Ia-DP4[c]				15:85:0
	IIa	**0.99908**[e]	**0.04**	**0.04**	**35**:**28**:**37**
	IIa-DP4				16:58:26
	Ia/IIa-DP4				5:95:0
	IIIb	0.99981	[0.08]	[0.10]	67.5:0:32.5
	IIIc	0.99966	[0.08]	[0.15]	64.5:0:35.5
1c	Ia[c]	0.99966	0.64	0.87	23:77:0
	Ia-DP4[c]				3:93:4
	IIa	0.99937[f]	0.03[g]	0.04[g]	0:36.2:63.8
	IIa-DP4				16:0:84
	Ia/IIa-DP4				15:1:84
	IIIb	**0.99222**[f]	[**0.33**][g]	[**0.48**][g]	**28**:**52**:**20**
	IIIc	0.99004[f]	[0.26][g]	[0.59][g]	24:53:23

[a] For the options **a** and **b** of methods **I** (δ_C), **II** (δ_H), and **III** (J_{HH}), see Table 6 and Computational details.
[b] In ppm or [Hz].
[c] The lactam group C=Y was omitted.
[d] Final least-squares fit equation of the form: δ_H^{scaled} [ppm]=(δ_H^{calcd}+0.2511)/1.0587.
[e] Final least-squares fit equation: δ_H^{scaled} [ppm]=(δ_H^{calcd}+0.2711)/1.0635.
[f] The low value most likely owing to strong degeneration of the experimental ^{1}H NMR data.
[g] The high value most likely owing to strong degeneration of the experimental ^{1}H NMR data.

It should be noted that η_Js analogously computed for isostructural systems **1a** and **1b** in $CHCl_3$ were a lot more unsatisfactory, independent from the calculational level used. However, their equatorial forms **A** and **B** have very similarly predicted J_{HH}-couplings, and so their differentiation was practically impossible. Hence, the predominant form **A** was only 'seen' in the analysis though both these forms should be recognized. As a result, such computed percentage of **A** should be considered as a total participation of the equatorial forms. Fortunately, it was not fully true for η_Js derived for 'solvates' of the thio system **1b** in more polar $(CH_3)_2CO$; 12–34% agreement, **A**:**B**:**C** ~47:21:32, CMAE=0.13 Hz (Table 3).

As for unsuccessful δ_C-based computations of ηs (also, using the DP4 algorithm,[12e] vide infra), such findings for **1a**–**c** generally show a lot worse agreement with the η_Gs or good-quality η_H/η_J data, despite very high magnitudes of r^2 factors obtained in a linear regression analysis. In particular, the negligible presence of forms **A** at the expense of forms **B** erroneously calculated for all systems **1a**–**c** at the DZ-level (and total lack of their forms **C** found at the TZ-level) should be noted. The best method applied here for predicting the δ_Cs comprise use of the WC04 density functional in $CHCl_3$ solution.[15e] However, we found, this approach not very reliable also for other molecular systems.[48,49] In fact, a comparatively large value of SD (2.2 ppm) determined in our check calculations could be a reason for such failure. Maybe, the proposed recently multi-standard approach for GIAO calculations,[35] with an application of benzene as an NMR reference for the sp^2-hybridized carbon atoms, would improve the agreement. On the other hand, very similar situation concerning unreliability of the δ_C-predictions was reported recently by Koskowich et al.[54] Thus, δ_Cs in vacuo computed by the B3LYP/6-311++G(*d*,*p*)//B3LYP/6-31G(*d*) method were not useful for trivial structure assignment of the tricyclic (with no sp^2 carbons, but with an ether oxygen atom) product studied by these authors, however the δ_H-based results were.

2.6. Verification of some η results by the DP4 probability analysis

All above NMR data-based findings on the mole fractions ηs of conformers **A**–**C** of **1a**–**c** were found by looking at the magnitudes of related r^2s, SDs, and CMAEs. However these indicators of correlations between the observation and experiment can be misleading, particularly when δ_Ks are strongly clustered into two groups as they really are in this work (see e.g., Fig. 3). Hence, for the purpose of additional validation of the ηs resulted from standard considerations of the δ_Ks, we also applied the new DP4 'probability' algorithm recommended recently by Smith and Goodman,[12e] as another tool assisted in important statistical handling of the aforementioned δ_K data.

In this fully automatic approach,[55] the 'corrected errors', i.e., differences $|<\delta_{Ki}>^{scaled}-<\delta_{Ki}>^{calcd}|$, are converted to the DP4 'probabilities' that these errors are obtained. More precisely, the theorem of Bayes as well as Student's *t*-distribution of such errors are inter alia applied. By repeating of this kind of calculations for all possible contributors being in fast equilibrium (e.g., conformers **A**–**C** of **1a**–**c**) their populations η_{DP4} can be supplied. This method also allows the ^{13}C and ^1H NMR data to be combined to give pertinent $\delta_{C,H}$-DP4 data. Originally,[12e] computationally inexpensive gas-phase MMFF94 geometries and B3LYP/6-31G(*d*,*p*) method were used in subsequent single-point in vacuo evaluations of energy and GIAO shieldings σ_Ks referenced finally to TMS, and the tool was parameterized just for such calculational conditions. Therefore, we also applied an identical protocol, for completeness. But, all so-obtained results (see Table S10 in Supplementary data) turned out to be a lot worse than those discussed before, especially for the system **1c** [**A**:**B**:**C** ~94:0:6 versus 37:27:36 or 28:52:20 (Tables 7 and 8)]. In other words, an original DP4 procedure[12e] is inadequate for the demanding objects under this study.

Thus, a deeper consideration of the DP4 results on selected good-quality δ_Ks concerning the systems **1** in $CHCl_3$ (i.e., δ_K-DP4 data, Tables 3, 5, and 8) led to a few conclusions. Firstly, as can easily see in Table 5, this method is also applicable in other similar cases [agreement within 11%, e.g., ±5.5%, with the B3LYP/6-31G(*d*) level (or a lot better) PCM/$CHCl_3$ GIAO δ_H-based predictions of ηs]. Indeed, very recently the DP4 analysis was successfully used in a comparable OPBE/pcS-1 PCM/$CHCl_3$//OPBE/6-31G(*d*) level study on the cyclopenta[*b*]benzofuran derivatives[56] and in the mPW1PW91/6-311+G(2*d*,*p*) PCM/$CHCl_3$//B3LYP/6-31+G(*d*,*p*) level correction of the structure of nobilisitine A.[18l] Secondly, the δ_H-DP4 data (η_{DP4}s) show the same or a little better agreement with the TZ-level η_Hs (Table 8) than with such results obtained at the DZ-geometries (Table 3), especially in the case of **1a** (1–6% vs 1–11%, for TZ and DZ, respectively). Thirdly, a reverse trend is observed for the δ_C-DP4s [in particular for **1c** (4–20% vs 2.5–18%, for the TZ and DZ-level data, respectively)], however, as we must remember, no correlation generally exists between η_Cs and η_Hs (or η_Gs). As a consequence, the (potentially best) combined $\delta_{C,H}$-DP4 results were found only minimally better from the δ_C-DP4s (Table 8).

All of the foregoing comparisons of different η results strongly suggest that only consideration of the enough reliable δ_H data computed for 'solvated' structures of the systems **1a**–**c** gives rational predictions on distributions of their conformers **A**–**C** (η_Hs), which are fully consistent with the populations η_Gs found from the temperature and *London forces* corrected Gibbs free energies (evaluated for 'solution', as well). Hence, an estimated uncertainty of such predictions of the η_Hs data with $r^2 \geq 0.9999$ seems to be about 5–10% or better. High reliability of such η_Hs, especially in the case of **1a**, was fully confirmed by a DP4 analysis. Regarding a little worse results η_H and η_{DP4} for lactams **1b** and **1c**, one can suppose that they arise, at least in part, from the greater *intramolecular London dispersion attraction* (mainly for **1b**, owing to the presence of an easily polarizable C=S bond) and larger conformational freedom (**1c**). The former effect strongly appeared in a large magnitude of the DFT-D3 term calculated for **1bC** (Table 7). As a consequence, the geometries of both these molecules and, therefore, their spectroscopic properties may be a little miscalculated. On the other hand, one ought to remember the strong degeneration of ^1H NMR data for **1c** (vide supra).

3. Summary and conclusions

In this work we have shown that three standard DFT methods initially used for an analysis of routine δ_C, δ_H, and J_{HH} NMR data for solution (embracing the GIAO-formalism-supported B3LYP calculations) led to the mutually incompatible results on fractional populations ηs of three fast interconverting low-energy forms **A**–**C** of the title systems **1a**–**c**, which were also inconsistent with their energies evaluated in a normal way. It should be stressed that all of such NMR-focused computational protocols, especially the first two δ_K-based tools, were applied previously[7c] with full success in elucidating relative configurations of rigid lactams **3** existing in equilibrium with a strong preference for the equatorial forms. Instead, the *J*-approach was used in an earlier work[9] on homologous bicycles **2** of a similar conformational behavior and so the use of popular Karplus-type equation[42] was sufficient in this case.

Generally, main difference between the two aforementioned series of molecules concerned their internal dynamics and the problems under investigation. Thus, a qualitative approach was satisfactory for the simple two-state equilibria and questions analyzed before (systems **2** and **3**), while an advanced, quantitative treatment was needed for reliable evaluating the populations ηs of three contributors **A**–**C** to conformational families of the highly-

flexible lactams **1** studied here. In other words, the more difficult problem demands the better tools.

Indeed, as a solution of the initial problem with the systems **1**, it was necessary to perform numerous computations with simultaneous modeling their solutions, by using the COSMO and/or IEF-PCM model. Specifically, the WC04/WP04 functionals and IGLO-II or IGLO-III basis sets were used, respectively, for predicting a lot of the δ_C/δ_H, and J_{HH} data needed for every of the individual equilibrating forms **A**–**C**. The vdW-DFT method was finally applied for crucial calculating their energies. It included an application of the double hybrid B2PLYP-D functional[51] introduced by Grimme with his DFT-D3 correction[44] to total energy for the *dispersion* (*London*) *interactions* not reproduced in conventional correlation functionals.[44,45] Thus, it was possible to collect the needed energetic data and, hence, to estimate mole fractions η_Gs of the forms **A**–**C**, which were consistent within 30% (or even ≤5% for **1a**) with the best NMR data-based results arising from the δ_H information (η_Hs).

In turn, the reliability of the GIAO-based and subsequent η results was estimated based on magnitudes of the determination coefficient, r^2, found in a linear regression analysis of predicted versus experimental data and on chemical intuition. Moreover, the recent DP4 'probability' method[12e] was also used in some cases as a second independent tool assisted in statistical evaluating the η data. This new DP4 protocol calculates a global probability from individual nucleus error probabilities and, therefore, it is especially useful in the analysis of various multiple isomeric entities in the equilibrium. The reliability of standard protocols was confirmed in this way, especially for **1a**. Thus, the most reliable η findings were obtained from the best correlations $<\delta_H^{calcd}>$ versus $<\delta_H>^{obsd}$ ($r^2>0.9996$, for **1a** and **1b**).

An analogous application of *J*-couplings for evaluating the populations ηs is possible only when there is a substantial differentiation of their values for individual conformers or favorable usage of the solvent. Indeed, the J_{HH} data computed for objects **1a**–**c** permitted only for sufficiently secure evaluation of the ratios of their equatorial versus axial forms, (**A**+**B**)/**C**, due to small differentiation of these data among both rotamers **A** and **B** (with some exceptions for **1b** and **1c**). However, the use of J_{HH}s, at least for control of an internal conformity of the predicted η_Hs, is strongly recommended when it is possible.

The best estimations of η_Hs or η_Js are consistent with the η_Gs treated as 'reference data' and all these NMR-based predictions are highlighted in Tables 3 and 8 (numbers in bold faces). Moreover, very good agreement between η_Hs and η_{DP4}s was found for **1a**, especially at the TZ level of approximation. Obviously, due to a semi-quantitative character of η_Gs, it is difficult to say which results (η_Gs, η_Hs, or $\delta_H-\eta_{DP4}$s) are really better, at this stage. An estimated uncertainty of such η_Hs seems to be ~5% or even better (at least for **1a**). Therefore, in this specific event one can speak about full alignment of the '*solution-phase environment* (i.e., NMR spectroscopic) *match criterion*' with the '*energetic criterion*'. However, both remaining molecules **1b** and **1c** were found to be more difficult cases. Undoubtedly, a great anisotropic effect of the phenyl ring existent in all studied systems, well known in the ^{1}H NMR spectroscopy, is responsible for very helpful differentiation of δ_Hs concerning their forms **A**–**C**. In sharp contrast, the use of similarly considered δ_C data for assessing the ηs was unsuccessful, despite high values of r^2 obtained in the regression analysis.

One can suppose, in line with the opinion of Sebag et al.,[4c] that in a vast majority of multi-conformer systems, where differences in the predicted values of NMR parameters among the possible equilibrating forms are substantial, the linear regression approach can, in principle, provide a fairly good approximation of the true conformational distributions ηs in solution. However, for this method to be a general tool, (1) the used computational protocol must be highly reliable, (2) all key forms must at least have unique sets of NMR quantities, and (3) all of the computations should be done for 'solution' applying adequate simulation of solvation. The rightness of all these criteria was confirmed in this work.

An unexpected failure in the estimation of mole fractions ηs for dynamic equilibria of the lactams **1** from GIAO-predicted δ_Cs deserves some comment. Calculations of δ_Cs in explicit solvents are nowadays in common use for numerous of (bio)organic molecules. But, the conclusions drawn using this type of NMR predictions are rather of qualitative nature, e.g., about their relative configurations and/or conformational preferences. So, an accuracy of standard computations of δ_Cs is sufficient for such purposes. However, their reliability was crucial for the present investigation.

Evidently, the GIAO-B3LYP differentiation of the δ_C sets for two rotamers **A** and **B** of systems **1a**–**c** and, especially, an accessible accuracy (not precision) of this tool was not sufficient. Indeed, an importance of the proper reproduction of *dispersion-type electron correlation interactions* for the computational results was highlighted several times throughout this work. Accordingly, no deeper discussion on the advantage of δ_H over δ_C or *J* data for evaluation of the ηs is possible, at this stage. In reality, every type of the molecular systems demands currently its suitable NMR-based approach. Interestingly, a superiority of the results from GIAO-predicted δ_Hs over analogous δ_C data, which was clearly shown here, has its own predecessor reported recently by Koskowich et al.[54]

Regarding the basis sets used in geometry pre-optimizations for NMR studies on the multitude of various interconverting conformers, it seems that use of the 6-31G(*d*) or equivalent basis set in conjunction with the B3LYP functional are sufficient for modeling their solvated structures. However, all subsequent NMR calculations demand rather TZ-level sets. In contrast, for evaluating the energies of such conformationally flexible entities, advanced computations at the TZ-level embracing suitable corrections (in particular, for *London forces*) are necessary. We hope that our conclusions will be useful as guidelines for the other NMR studies, especially those concerning the multi-conformer systems in rapid equilibrium between more than two forms energetically feasible in solution.

4. Experimental

4.1. Materials

All studied systems **1** are known compounds;[7] **1b** and **1c** have recently been described for the first time in Ref. 7c. In this synthetic work, all used procedures of separation/purification of the products, and their standard characterizations were presented in detail. Some new NMR spectroscopic data and/or full assignments of the signals previously reported are given in Table 1 (^{1}H NMR) or below.

*4.1.1. 1-Methyl-4-phenyl-pyrrolidin-2-one (**1a**).* δ_C (50.3 MHz, $CDCl_3$) 173.84 (*C*=O), 142.55 (C_{ipso}), 128.87 (C_{meta}), 127.05 (C_{para}), 126.71 (C_{ortho}), 56.67 (*C*5H$_2$), 38.80 (*C*3H$_2$), 37.15 (*C*4H), 29.57 (N*Me*).

*4.1.2. 1-Methyl-4-phenyl-pyrrolidin-2-thione (**1b**).* δ_C (50.3 MHz, $CDCl_3$) 200.30 (*C*=S), 141.57 (C_{ipso}), 128.99 (C_{meta}), 127.27 (C_{para}), 126.68 (C_{ortho}), 63.85 (*C*5H$_2$), 52.17 (*C*3H$_2$), 38.85 (*C*4H), 35.43 (N*Me*); δ_C [50.3 MHz, $(CD_3)_2CO$] 200.66 (*C*=S), 143.51 (C_{ipso}), 129.70 (C_{meta}), 127.80$_5$ (C_{para}), 127.78$_5$ (C_{ortho}), 63.86 (*C*5H$_2$), 53.04 (*C*3H$_2$), 39.62 (*C*4H), 35.26 (N*Me*).

*4.1.3. 4-Benzoyl-1-methyl-pyrrolidin-2-one (**1c**).* δ_H (200.0 MHz, $CDCl_3$, only aromatic Hs) 7.95 (pdt, 2H, C*H*$_{ortho}$), 7.63 (ptt, 1H, C*H*$_{para}$), 7.51 (ptt, 2H, C*H*$_{meta}$); δ_C (50.3 MHz, $CDCl_3$) 198.07 (*C*=O$_{ketone}$), 172.43 (*C*=O$_{amide}$), 133.92 (C_{para}), 133.33 (C_{ipso}), 129.11

(C_{ortho}), 128.65 (C_{meta}), 50.70 ($C5H_2$), 38.12 ($C4H$), 34.19 ($C3H_2$), 29.60 (N*Me*).

4.2. NMR spectroscopy

The $^1H/^{13}C$ NMR spectra were collected on a Varian Gemini-200 BB spectrometer operating at nominal frequencies of 199.98/50.29 MHz for the ^1H and ^{13}C nuclei, respectively. $CDCl_3$ was used as a solvent unless stated otherwise. All measurements were taken at a probe temperature (~21 °C). Chemical shifts δ_Ks (K=H, C) are expressed in parts per million against internal tetramethylsilane (TMS), while coupling constants $^nJ_{HH}$ are given in Hz. Signals are reported as s (singlet), d (doublet), t (triplet), q (quartet), (multiplet), br (broad), c (center) or p (pseudo). 128–256 transients were usually accumulated for ^1H NMR spectra using the spectral width of 2.5 kHz. The obtained 32 K time-domain spectra were zero-filled to 64 K data point sets and additionally resolution enhanced with the Lorentzian-to-Gaussian function,[31] prior to the Fourier transformation. Optimal values of two parameters for this improvement method, i.e., AF and RE, were selected by a trial-and-error procedure available as a post-processing option within standard Varian software. The final digital resolution of such improved frequency-domain ^1H NMR spectra was ≤0.08 Hz. An unambiguous assignment of observed NMR signals, which was crucial for the successful completion of conformational analysis, was accomplished on the basis of selective decouplings and/or the combined inspection of additional spectra (ATP, DEPT, H,H-COSY, and C,H-HETCOR).

4.3. Computational details

4.3.1. Molecular modeling and vibrational frequency calculations. A full conformational search for the minima on PESs of the isolated molecules of systems **1** was initially performed with the MMX force field molecular-mechanics calculations, by using the Monte Carlo (MC)-type GMMX subroutine embedded within PCMODEL Version 8.5.[57] A mixed molecular-mechanics searching protocol was employed with the randomization over all rotatable bonds.[58] Typically, ~1000 MC steps were employed within the 14.6 kJ mol^{-1} threshold (energy window); a bulk value of the relative permittivity (dielectric constant) being applied for the gas phase, ε=1.50.[59] The ensuing varieties of so-obtained energetically preferred MMX structures were subsequently used as trial input configurations in the geometrical optimization carried out with the semi-empirical PM3 hamiltonian of HyperChem.[60] The resulting low-energy molecular models were subjected next to further fully-relaxed geometry refinement at the ab initio restricted HF level of theory, by using two standard Pople's split-valence one-electron basis sets, i.e., initially 3-21 G[33b] and than 6-31G(*d*) (with the six, not five, *d*-like Gaussian functions employed for all non-H atoms) within the Gaussian 03 package of programs.[47] Final gas-phase energy minimizations were carried out with the Berny algorithm applying standard 6-31G(*d*) [or 6-31G(*d*,*p*)] basis set in conjunction with a combination of Becke's three-parameter exchange functional[61] and Lee-Yang-Parr correlation functional[62] (B3LYP) as it was implemented[19] in the Gaussian code.

For the DP4 'probability' analysis,[12e] geometries of all nine major forms **A**–**C** of the objects **1a**–**c** were in vacuo assessed within PCMODEL,[57] by applying the MMFF94 force field[63] and ε=1.0. Their gas-phase energies were evaluated at the B3LYP6-31G(*d*,*p*) level. Selected results are given in Table S10.

All of the molecular energy minima were found without any symmetry constraints (C_1 point group), by optimizing the equilibrium configurations with the help analytical gradients and using an 'ultrafine' pruned grid having 99 radial shells and 590 angular points per shell (99,590); keyword: Int(Grid=UltraFine).[64] In almost all cases, the final steps of calculations had to be run applying the GDIIS (geometry optimization using direct inversion in the iterative subspace) algorithm[18f,65] Also attempts to evaluate solvent influence on the molecular structures and properties were made, by using an SCRF model. Specifically, an integral equation-formalism polarizable continuum model (IEF-PCM)[17] technique was applied at 298.15 K for $CHCl_3$ and $(CH_3)_2CO$, within Gaussian 03. The in vacuo pre-optimized geometries and default values of ε=4.90 and 20.70 were used, respectively. Solute cavities for such modeling the solutions in $CHCl_3$ were constructed as a sum of atom-centered spheres employing the atomic radii of Bondi[15e,66] or default united-atom (UA0) radii;[18g] see also text and Ref. 50.

Moreover, vibrational wavenumbers, ω_i, were computed for several structures (in the gas phase or solution state) in the rigid rotor-harmonic oscillator approximation of vibrational modes according to the G–F method of Wilson,[67] by using the analytic second derivatives. These data were used to verify that all located stationary points represented the true potential energy minima on DFT Born–Oppenheimer PESs (N_{imag}=0) and to determine the relative standard Gibbs free energies of conformers at 298.15 K, ΔG°_{298},[27] i.e., close to the NMR recording temperature of ~294 K. The needed zero-point energies (*ZPE*s) were estimated from the B3LYP/6-31G(*d*) harmonic frequencies ω_i uniformly scaled with an arbitrary averaged factor of 0.97.[28] It is known[28d] that this transferable global scale factor is slightly above 0.96±0.02[28a,e] recommended, at this level of approximation, to reproduce experimental fundamentals, ν_i.

All of the DZ-level optimized 'solvated' ($CHCl_3$) structures **1a**–**c** were subjected next to an additional geometry optimization at the TZ-level within the PC version of an ORCA suite of programs.[46a] The hybrid B3PLYP/G functional in conjunction with a basis set of triple-ζ valence quality augmented with one set of polarization functions (def2-TZVP)[68,69] was used for this purpose, while related solvent effects were simulated through the COSMO solvation model[23] with $CHCl_3$ parameters; keywords: TightOpt, Grid4, and VeryTightSCF. Subsequent single-point energy refinements were performed employing the doubly hybrid B2PLYP-D functional[51] and doubly polarized def2-TZVPP basis set,[68] with additional *d*/*f* and *p*/*d* functions on the non-H and H-atoms, respectively. The COSMO technique and Grimme's latest correction to total DFT energy for dispersion-type interactions[44,45] were employed (DFT-D3 method).[44] In order to speed up all of these additional calculations, the resolution-of-the-identity (RI) approximation[70] for two-electron integrals was used as implemented in ORCA. Matching RI auxiliary basis functions, def2-TZVPP/C, were taken from the TURBOMOLE basis sets library.[71] Always, five spherical-harmonic Gaussian-type polarization functions were applied for all basis sets, as opposed to six Cartesian *d*-like gaussians used with the Gaussian program.

For assessing the fractional population (mole fraction, η_{Gi}) of each conformer, where j is the number of forms within each equilibrium, the Boltzmann distribution function $\eta_{Gi} = e^{-\Delta Gi^0/RT} / \sum_j e^{-\Delta Gj^0/RT}$ was used, where R is the ideal gas constant, T is the absolute temperature set to 298.15 K, and ΔG_i^0 is the standard Gibbs free energy value of the ith form relative to the energy of the most stable conformer.

4.3.2. NMR calculations (of chemical shifts and J-couplings). Initial single-point GIAO[1] formalism-based computations of absolute values of isotropic shielding constants (σ_Ks) were executed at the B3LYP/6-31G(*d*) level on fully relaxed B3LYP/6-31G(*d*) structures, by using standard routines in the Gaussian 03 package.[47] The 'tight' SCF convergence criterion was always applied.[2b,39] The relative chemical shift δ_K of a given nucleus K in each entity was defined as $\delta_K{}^{calcd}$ [ppm]=$\sigma_K{}^{ref}-\sigma_K{}^{calcd}$. In the case of so-predicted ^1H and ^{13}C NMR spectra, $\sigma_K{}^{ref}$ was of 32.1821, 32.1694, 32.1671, and 31.8338 ppm as well as of 189.7709, 189.9824, 190.0905, and 192.3560 ppm as was

found for the three B3LYP/6-31G(*d*) and one gas-phase MMFF94 models of a dual-reference δ_K standard (TMS, T_d point group, 'opt=tight')[27a] in vacuum, $CHCl_3$ or $(CH_3)_2CO$ (both solutions simulated by the IEF-PCM method)[17] and in vacuum, respectively. Several other combinations of the functional (B3LYP, WC04[15e] or WP04[15e]) and basis set [6-31G(*d*,*p*) or 6-311+G(2*d*,*p*)] were used in some additional calculations for the gaseous or solution state (see text, Tables 3, 5, and 6); the last two functionals were executed as a modification of B3LYP with an 'iop' statement.[15e] All of these runs were performed at the structures fully pre-optimized at the DZ or TZ level of theory (see above). The σ_K^{calcd}s computed in this way were, as above, referred to TMS, by using adequate σ_K^{ref} terms evaluated at the same calculational level.

Moreover, indirect interproton coupling constants, $^nJ_{HH}$, were predicted for the gaseous [or solution] state of systems **1** or **4** by the {B3LYP/IGLO-II (or IGLO-III) [IEF-PCM (solvent)]//DZ or TZ-level optimized structure [IEF-PCM (solvent) or COSMO (solvent)]} method[41] within Gaussian 03, which allows for computations of all four Ramsey's contributions to the *J*-couplings. In these *J*-predictions two extended basis sets commonly called IGLO-II and IGLO-III[22e,f] were applied. These bases (also known as HII/III or BII/III basis sets) originally due to Huzinaga,[72] were modified by van Wüllen, Kutzelnigg et al.[22a,b] through addition of polarization functions and contraction patterns. Both IGLO bases include more tight functions (particularly of *s* symmetry) than standard extended basis sets and thus they are more flexible in the neighborhood of nucleus, i.e., the region relevant for the description of NMR properties. In these *J*-calculations, the five 'pure *d*' type basis functions were employed for all non-H atoms.

The calculated nuclear shieldings each of the three mutually exchanging hydrogens in Me groups of the systems **1** and **4** were arithmetically averaged to produce a single observable value for the Me group as a whole. Similar procedure was used also in relation to the Ph groups (pairwise exchange of *ortho* and *meta* $^1H/^{13}C$ nuclei). The J_{HH}-couplings involving Me groups were found analogously. A linear regression analysis of the dependence between experimental and calculated NMR parameters has been achieved by least-squares method. All statistical analysis was carried out with the Excel spreadsheet. The greater value of the correlation coefficient of Pearson, *r*, [or its square (also called determination coefficient), r^2, which shows the correlation significance] was usually considered as an indication of the better adjustment of correlated data sets. The molecules were visualized applying the graphical representation of ChemCraft.[29]

Note added in proof

The other molecule fulfilling the aforementioned '*solution-phase environment match criterion*' and not an '*energetic criterion*' was reported by Alcântara *et al.*[74] [a boat conformer of **8**, adequate J_{HH}^{obsd}s and δ_K^{calcd}s consistent with δ_K^{obsd}s (K = C, H) *versus* the B3LYP/6-31G(*d*)-computed ΔGs]. In turn, an analogous (to this shown here in Table 7) evaluation of relative B2PLYP-D/cc-pVDZ-level Gibbs free energies, ΔGs, based on the B3LYP/6-31(*d*) thermal corrections has just been published.[75]

Acknowledgements

This work was supported in part by the calculation facilities and Gaussian 03 software in the Supercomputing and Networking Center CYFRONET (AGH, Kraków, Poland) through thecomputational grants Nos. MNiSW/SGI3700/UŁódzki/053/2009 and /057/2010. The authors also thank an anonymous reviewer who pointed out some references that had been missed in their original literature search.

Supplementary data

TZ-level Cartesian coordinates of all nine solvated forms **A**–**C** of the objects **1a**–**c** and related results (the angles θ, energies and η_{DP4}s) obtained in accord with an original DP4 protocol (Tables S1–S10) (11 pages, PDF). Supplementary data associated with this article can be found in the online version, at doi:10.1016/j.tet.2011.06.095. These data include MOL files and InChiKeys of the most important compounds described in this article.

References and notes

1. For a comprehensive list of references see Aminova, R. M.; Schamov, G. A.; Aganov, A. V. *J. Mol. Struct. (Theochem)* **2000**, *498*, 233–246 and Refs 30–41 cited therein.
2. (a) Helgaker, T.; Jaszuński, M.; Ruud, K. *Chem. Rev.* **1999**, *99*, 293–352; (b) Tähtinen, P.; Bagno, A.; Klika, K. D.; Pihlaja, K. *J. Am. Chem. Soc.* **2003**, *125*, 4609–4618 and refs therein; (c) *Calculation of NMR and EPR Parameters. Theory and Applications*; Kaupp, M., Bühl, M., Malkin, V. G., Eds.; Wiley-VCH: Weinheim, Germany, 2004; (d) Helgaker, T.; Jaszuński, M.; Pecul, M. *Prog. Nucl. Magn. Reson. Spectrosc.* **2008**, *53*, 249–268 and refs therein.
3. (a) Michalik, E.; Nazarski, R. B. *Tetrahedron* **2004**, *60*, 9213–9222; (b) Nazarski, R. B. *J. Phys. Org. Chem.* **2009**, *22*, 834–844; (c) Nazarski, R. B. *Tetraazacyclotetradecane Species as Models of the Polyazacrown Macrocycles (Chemistry Research and Applications Series)*; Nova Science: New York, NY, 2010, pp 46–48.
4. See e.g., (a) Forsyth, D. A.; Sebag, A. B. *J. Am. Chem. Soc.* **1997**, *119*, 9483–9494 and refs therein; (b) Sebag, A. B.; Friel, C. J.; Hanson, R. N.; Forsyth, D. A. *J. Org. Chem.* **2000**, *65*, 7902–7912; (c) Sebag, A. B.; Forsyth, D. A.; Plante, M. A. *J. Org. Chem.* **2001**, *66*, 7967–7973; (d) Bouř, P.; Sychrovský, V.; Maloň, P.; Hanzlíková, J.; Baumruk, V.; Pospíšek, J.; Buděšinský, M. *J. Phys. Chem. A* **2002**, *106*, 7321–7327; (e) Barone, G.; Duca, D.; Silvestri, A.; Gomez-Paloma, L.; Riccio, R.; Bifulco, G. *Chem.—Eur. J.* **2002**, *8*, 3240–3245; (f) Cimino, P.; Bifulco, G.; Evidente, A.; Abouzeid, M.; Riccio, R.; Gomez-Paloma, L. *Org. Lett.* **2002**, *4*, 2779–2782 and refs therein; (g) Migda, W.; Rys, B. *J. Org. Chem.* **2006**, *71*, 5498–5506; (h) Fattorusso, C.; Stendardo, E.; Appendino, G.; Fattorusso, E.; Luciano, P.; Romano, A.; Taglialatela-Scafati, O. *Org. Lett.* **2007**, *9*, 2377–2380; (i) Belostotskii, A. M. *J. Org. Chem.* **2008**, *73*, 5723–5731; (j) Fattorusso, E.; Luciano, P.; Romano, A.; Taglialatela-Scafati, O.; Appendino, G.; Borriello, M.; Fattorusso, C. *J. Nat. Prod.* **2008**, *71*, 1988–1992.
5. (a) Cygler, M.; Dobrynin, K.; Grabowski, M. J.; Nazarski, R. B.; Skowroński, R. *J. Chem. Soc., Perkin Trans. 2* **1985**, 1495–1501; (b) Nazarski, R. B.; Skowroński, R. *Pol. J. Chem.* **2003**, *77*, 415–426.
6. (a) Sroczyński, D.; Grzejdziak, A.; Nazarski, R. B. *J. Inclusion Phenom. Macrocyclic Chem.* **1999**, *35*, 251–260; (b) Nazarski, R. B. *Magn. Reson. Chem.* **2003**, *41*, 70–74 and refs therein.
7. (a) Pasternak, B. Ph.D. Thesis, University of Łódź, Łódź, 2002; (b) Leśniak, S.; Pasternak, B. *Tetrahedron Lett.* **2005**, *46*, 3093–3095; (c) Leśniak, S.; Nazarski, R. B.; Pasternak, B. *Tetrahedron* **2009**, *65*, 6364–6369.
8. These results on the isostructural systems **1a** and **1b** were presented at the VIIIth Polish Symposium on Organic Chemistry, April 10–12, 2008, Łódź, Poland; Abstracts, poster P 69.
9. Nazarski, R. B.; Leśniak, S. *Bull. Pol. Acad. Sci., Chem.* **2000**, *48*, 19–25 and refs therein.
10. Barone, G.; Gomez-Paloma, L.; Duca, D.; Silvestri, A.; Riccio, R.; Bifulco, G. *Chem.—Eur. J.* **2002**, *8*, 3233–3239 and refs therein.
11. (a) Matsumori, N.; Murata, M.; Tachibana, K. *Tetrahedron* **1995**, *51*, 12229–12238; (b) Matsumori, N.; Kaneno, D.; Murata, M.; Nakamura, H.; Tachibana, K. *J. Org. Chem.* **1999**, *64*, 866–876 and refs therein.
12. See e.g., (a) Bassarello, C.; Cimino, P.; Gomez-Paloma, L.; Riccio, R.; Bifulco, G. *Recent Res. Dev. Org. Chem.* **2003**, *7*, 219–239; (b) Bifulco, G.; Dambruoso, P.; Gomez-Paloma, L.; Riccio, R. *Chem. Rev.* **2007**, *107*, 3744–3779; (c) Smith, S. G.; Goodman, J. M. *J. Org. Chem.* **2009**, *74*, 4597–4607; (d) Di Micco, S.; Chini, M. G.; Riccio, R.; Bifulco, G. *Eur. J. Org. Chem.* **2010**, 1411–1434; (e) Smith, S. G.; Goodman, J. M. *J. Am. Chem. Soc.* **2010**, *132*, 12946–12959.
13. (a) Malkina, O. L.; Salahub, D. R.; Malkin, V. G. *J. Chem. Phys.* **1996**, *105*, 8793–8800; (b) Stahl, M.; Schopfer, U.; Frenking, G.; Hoffmann, R. W. *J. Org. Chem.* **1997**, *62*, 3702–3704; (c) Sychrovský, V.; Gräfenstein, J.; Cremer, D. *J. Chem. Phys.* **2000**, *113*, 3530–3547; (d) Bagno, A. *Chem.—Eur. J.* **2001**, *7*, 1652–1661 and refs therein; (e) Bagno, A.; Rastrelli, F.; Saielli, G. *J. Phys. Chem. A* **2003**, *107*, 9964–9973.
14. (a) Wu, A.; Cremer, D.; Auer, A. A.; Gauss, J. *J. Phys. Chem. A* **2002**, *106*, 657–667; (b) Wu, A.; Cremer, D. *Int. J. Mol. Sci.* **2003**, *4*, 158–192.
15. See e.g., chemical shifts: (a) Baldridge, K. K.; Siegel, J. S. *J. Phys. Chem. A* **1999**, *103*, 4038–4042; (b) Colombo, D.; Ferraboschi, P.; Ronchetti, F.; Toma, L. *Magn. Reson. Chem.* **2002**, *40*, 581–588; (c) Migda, W.; Rys, B. *Magn. Reson. Chem.* **2004**, *42*, 459–466; (d) Cimino, P.; Gomez-Paloma, L.; Duca, D.; Riccio, R.; Bifulco, G. *Magn. Reson. Chem.* **2004**, *42*, S26–S33; (e) Wiitala, K. W.; Hoye, T. R.; Cramer, C. J. *J. Chem. Theory Comput.* **2006**, *2*, 1085–1092; (f) Refs. 21–29 cited in the Ref. 12c; (g) Jensen, F. *J. Chem. Theory Comput.* **2008**, *4*, 719–727; (h) Jain, R.; Bally, T.; Rablen, P. R. *J. Org. Chem.* **2009**, *74*, 4017–4023; (i) Kupka, T.; Stachów, M.; Nieradka, M.; Kaminsky, J.; Pluta, T. *J. Chem. Theory Comput.* **2010**, *6*, 1580–1589 *J*-couplings: (j) Jensen, F. *J. Chem. Theory Comput.* **2006**, *2*,

1360–1369 and refs therein; (k) Kupka, T. *Magn. Reson. Chem.* **2009**, *47*, 674–683.
16. Traditionally, so-called 'gas-phase' calculations refer to isolated vibration-free molecules at 0 K in vacuum (free space).
17. (a) Mennucci, B.; Tomasi, J. *J. Chem. Phys.* **1997**, *106*, 5151–5158; (b) Cancès, E.; Mennucci, B.; Tomasi, J. *J. Chem. Phys.* **1997**, *107*, 3032–3041; (c) Mennucci, B.; Cancès, E.; Tomasi, J. *J. Phys. Chem. B* **1997**, *101*, 10506–10517; (d) Cossi, M.; Barone, V.; Mennucci, B.; Tomasi, J. *Chem. Phys. Lett.* **1998**, *286*, 253–260; (e) Tomasi, J.; Mennucci, B.; Cancès, E. *J. Mol. Struct. (Theochem)* **1999**, *464*, 211–226.
18. (a) Chesnut, D. B. In *The Ab Initio Computation of Nuclear Magnetic Resonance Chemical Shielding*; Lipkowitz, K. B., Boyd, D. B., Eds.; Reviews in Computational Chemistry; VCH: New York, NY, 1996; Vol. 8, pp 245–297; (b) Barfield, M.; Fagerness, P. *J. Am. Chem. Soc.* **1997**, *119*, 8699–8711; (c) Ośmiałowski, B.; Kolehmainen, E.; Gawinecki, R. *Magn. Reson. Chem.* **2001**, *39*, 334–340; (d) van Eikema Hommes, N. J. R.; Clark, T. *J. Mol. Model.* **2005**, *11*, 175–185; (e) Aiello, A.; Fattorusso, E.; Luciano, P.; Mangoni, A.; Menna, M. *Eur. J. Org. Chem.* **2005**, 5024–5030; (f) Bagno, A.; Rastrelli, F.; Saielli, G. *Chem.—Eur. J.* **2006**, *12*, 5514–5525 and refs therein; (g) Wiitala, K. W.; Cramer, C. J.; Hoye, T. R. *Magn. Reson. Chem.* **2007**, *45*, 819–829 and refs therein; (h) Smith, S. G.; Paton, R. S.; Burton, J. W.; Goodman, J. M. *J. Org. Chem.* **2008**, *73*, 4053–4062; (i) Dybiec, K.; Gryff-Keller, A. *Magn. Reson. Chem.* **2009**, *47*, 63–66 and refs therein; (j) Aliev, A. E.; Courtier-Murias, D.; Zhou, S. *J. Mol. Struct. (Theochem)* **2009**, *893*, 1–5; (k) Pankratyev, E. Y.; Tulyabaev, A. R.; Khalilov, L. M. *J. Comput. Chem.* **2011**, *32*, 1993–1997; (l) Lodewyk, M. W.; Tantillo, D. J. *J. Nat. Prod.* **2011**, *74*, 1334–1343 and refs therein.
19. (a) Stephens, P. J.; Devlin, F. J.; Chabalowski, C. F.; Frisch, M. J. *J. Phys. Chem.* **1994**, *98*, 11623–11627 and refs therein; (b) Cheeseman, J. R.; Truck, G. W.; Keith, T. A.; Frisch, M. J. *J. Chem. Phys.* **1996**, *104*, 5497–5509.
20. (a) Claramunt, R. M.; López, C.; Sanz, D.; Alkorta, I.; Elguero, J. *Heterocycles* **2001**, *55*, 2109–2121 and refs therein; (b) Leśniak, S.; Chrostowska, A.; Kuc, D.; Maciejczyk, M.; Khayar, S.; Nazarski, R. B.; Urbaniak, Ł. *Tetrahedron* **2009**, *65*, 10581–10589.
21. Lampert, H.; Mikenda, W.; Karpfen, A.; Kähling, H. *J. Phys. Chem. A* **1997**, *101*, 9610–9617.
22. (a) Schindler, M.; Kutzelnigg, W. *J. Chem. Phys.* **1982**, *76*, 1919–1933; (b) Kutzelnigg, W.; Fleischer, U.; Schindler, M. In *NMR—Basic Principles and Progress (Deuterium and Shift Calculation)*; Diehl, P., Fluck, E., Günther, H., Kosfeld, R., Seelig, J., Eds.; Springer: Berlin, 1991; Vol. 23, pp 165–262; (c) Ruud, K.; Helgaker, T.; Kobayashi, R.; Jørgensen, P.; Bak, K. L.; Jensen, H. J. A. *J. Chem. Phys.* **1994**, *100*, 8178–8185; (d) Ruden, T. A.; Lutnæs, O. B.; Helgaker, T.; Ruud, K. *J. Chem. Phys.* **2003**, *118*, 9572–9581 and refs therein; (e) Basis sets were obtained from the Extensible Computational Chemistry Environment Basis Set Database, Version 02/25/2004, as developed and distributed by the Molecular Science Computing Facility, Environmental and Molecular Sciences Laboratory which is part of the Pacific Northwest Laboratory, P.O. Box 999, Richland, WA 99352, USA, and funded by the U.S. Department of Energy. The Pacific Northwest Laboratory is a multiprogram laboratory operated by Battelle Memorial Institute for the U.S. Department of Energy under contract DE-AC06-76RLO 1830. Contact Karen Schuchardt for further information; (f) EMSL Basis Set Library; https://bse.pnl.gov/bse/portal; (g) Schuchardt, K. L.; Didier, B. T.; Elsethagen, T.; Sun, L.; Gurumoorthi, V.; Chase, J.; Li, J.; Windus, T. L. *J. Chem. Inf. Model.* **2007**, *47*, 1045–1052.
23. (a) Klamt, A.; Schüürmann, G. *J. Chem. Soc., Perkin Trans. 2* **1993**, 799–805; (b) Klamt, A.; Jonas, V.; Bürger, T.; Lohrenz, J. C. W. *J. Phys. Chem. A* **1998**, *102*, 5074–5085; (c) Chipman, D. M. *Theor. Chem. Acc.* **2002**, *107*, 80–89 and refs therein; (d) Sinnecker, S.; Rajendran, A.; Klamt, A.; Diedenhofen, M.; Neese, F. *J. Phys. Chem. A* **2006**, *110*, 2235–2245.
24. (a) Rayón, V. M.; Sordo, J. A. *J. Chem. Phys.* **2005**, *122*, 204303-1–204303-8; (b) Duffy, P.; Sordo, J. A.; Wang, F. *J. Chem. Phys.* **2008**, *128*, 125102-1–125102-10.
25. (a) Kuppens, T.; Vandyck, K.; van der Eycken, J.; Herrebout, W.; van der Veken, B.; Bultinck, P. *Spectrochim Acta A* **2007**, *67*, 402–411 (VCD data); (b) Kwit, M.; Rozwadowska, M. D.; Gawroński, J.; Grajewska, A. *J. Org. Chem.* **2009**, *74*, 8051–8063 (ECD data).
26. Sato, T.; Chono, N.; Ishibashi, H.; Ikeda, M. *J. Chem. Soc., Perkin Trans. 1* **1995**, 1115–1120.
27. (a) Foresman, J. B.; Frisch, Æ. *Exploring Chemistry with Electronic Structure Methods*, 2nd ed.; Gaussian: Pittsburgh, PA 15106, 1996, Chapter 4+Errata; (b) Irikura, K. K. *Computational Thermochemistry: Prediction and Estimation of Molecular Thermodynamics*; Irikura, K. K., Frurip, D. J., Eds. ACS Symposium Series 677; American Chemical Society: Washington, DC, 1998, Appendix B. Essential Statistical Thermodynamics (Errata corrected through January 19, 2001).
28. (a) Scott, A. P.; Radom, L. *J. Phys. Chem.* **1996**, *100*, 16502–16513 and refs therein; (b) Curtiss, L. A.; Raghavachari, K.; Redfern, P. C.; Pople, J. A. *Chem. Phys. Lett.* **1997**, *270*, 419–426 and refs therein; (c) Barone, V. *J. Chem. Phys.* **2004**, *120*, 3059–3065; (d) Sinha, P.; Boesch, S. E.; Gu, C.; Wheeler, R. A.; Wilson, A. K. *J. Phys. Chem. A* **2004**, *108*, 9213–9217; (e) Irikura, K. K.; Johnson, R. D., III; Kacker, R. N. *J. Phys. Chem. A* **2005**, *109*, 8430–8437.
29. Chemcraft, Version 1.6 (built 338); http://www.chemcraftprog.com.
30. Smith, S. L. *Top. Curr. Chem.* **1972**, *27*, 117–187.
31. See, e.g., (a) Ferrige, A. G.; Lindon, J. C. *J. Magn. Reson.* **1978**, *31*, 337–340; (b) Lindon, J. C.; Ferrige, A. G. *Prog. Nucl. Magn. Reson.* **1980**, *14*, 27–66; (c) Kupka, T.; Dzięgielewski, J. O. *Magn. Reson. Chem.* **1988**, *26*, 353–357; (d) Anet, F. A.; O'Leary, D. J. *Tetrahedron Lett.* **1989**, *30*, 2755–2758.
32. Chapman, O. L.; Hoganson, E. D. *J. Am. Chem. Soc.* **1964**, *86*, 498–500.
33. (a) Maciel, G. E.; McIver, J. W., Jr.; Ostlund, N. S.; Pople, J. A. *J. Am. Chem. Soc.* **1970**, *92*, 1–11 (INDO approximation); (b) Jiao, D.; Barfield, M.; Hruby, V. J. *J. Am. Chem. Soc.* **1993**, *115*, 10883–10887 (HF methods) and refs therein; (c) Ref. 13a DFT functionals; (d) Provasi, P. F.; Aucar, G. A.; Sauer, S. P. A. *J. Chem. Phys.* **2001**, *115*, 1324–1334 (ab initio SOPPA methods) and refs therein.
34. See, e.g., (a) Bifulco, G.; Gomez-Paloma, L.; Riccio, R. *Tetrahedron Lett.* **2003**, *44*, 7137–7141 (lactone carbonyl); (b) Ref. 4j lactone carbonyl; (c) Wang, B.; Dossey, A. T.; Walse, S. S.; Edison, A. S.; Merz, K. M., Jr. *J. Nat. Prod.* **2009**, *72*, 709–713 (ethylenic and carbonyl carbons).
35. Sarotti, A. M.; Pellegrinet, S. C. *J. Org. Chem.* **2009**, *74*, 7254–7260.
36. Poza, J. J.; Jiménez, C.; Rodríguez, J. *Eur. J. Org. Chem.* **2008**, 3960–3969.
37. See, e.g., (a) Note 65 in Ref. 3b N–C, HF/6-31(*d*,*p*); (b) Ref. 5b O–C, HF/6-31(*d*,*p*); (c) Braddock, D. C.; Rzepa, H. S. *J. Nat. Prod.* **2008**, *71*, 728–730 [O=C–O, Cl–C, and Br–C, DFT-mPW1PW91/6-31(*d*,*p*)]; (d) Ref. 18h Br–C and HC≡C, DFT-B3LYP/6–31(*d*,*p*).
38. Rychnovsky, S. D. *Org. Lett.* **2006**, *8*, 2895–2898.
39. Woodford, J. N.; Harbison, G. S. *J. Chem. Theory Comput.* **2006**, *2*, 1464–1475.
40. On the assumption of standard calculations of energies (HF or conventional DFT with a simulated solvation).
41. The successful use of the B3LYP/lGLO-II//B3LYP/6-31G(d) computational level for predicting the $^{n}J_{HH}$s in small-to-medium sized molecules was inter alia reported in (a) Dodziuk, H.; Jaszuński, M.; Schilf, W. *Magn. Reson. Chem.* **2005**, *43*, 639–646; (b) Ref.20b.
42. Haasnoot, C. A. G.; de Leeuw, F. A. A. M.; Altona, C. *Tetrahedron* **1980**, *36*, 2783–2792.
43. Kolehmainen, E.; Laihia, K.; Laatikainen, R.; Vepsäläinen, J.; Niemitz, M.; Suontamo, R. *Magn. Reson. Chem.* **1997**, *35*, 463–467.
44. Grimme, S.; Antony, J.; Ehrlich, S.; Krieg, H. *J. Chem. Phys.* **2010**, *132*, 154104-1–154104-19.
45. See, e.g., (a) Kristyán, S.; Pulay, P. *Chem. Phys. Lett.* **1994**, *229*, 175–180; (b) Cioslowski, J.; Liu, G.; Moncrieff, D. *J. Phys. Chem. A* **1998**, *102*, 9965–9969; (c) Grimme, S. *Angew. Chem., Int. Ed.* **2006**, *45*, 4460–4464 and refs therein; (d) Grimme, S. *J. Comput. Chem.* **2006**, *27*, 1787–1799; (e) Grimme, S.; Antony, J.; Schwabe, T.; Mück-Lichtenfeld, C. *Org. Biomol. Chem.* **2007**, *5*, 741–758 and refs therein; (f) Johnson, E. R.; Mackie, I. D.; DiLabio, G. A. *J. Phys. Org. Chem.* **2009**, *22*, 1127–1135; (g) Kannemann, F. O.; Becke, A. D. *J. Chem. Theory Comput.* **2010**, *6*, 1081–1088; (h) Song, J.-W.; Tsuneda, T.; Sato, T.; Hirao, K. *Org. Lett.* **2010**, *12*, 1440–1443; (i) Grimme, S. *Org. Lett.* **2010**, *12*, 4670–4673; (j) Sherrill, C. D. *J. Chem. Phys.* **2010**, *132*, 110902-1–110902-7 and refs therein; (k) Grimme, S.; Huenerbein, R.; Ehrlich, S. *ChemPhysChem* **2011**, *12*, 1258–1261.
46. Neese, F. and et al., ORCA—An ab initio, DFT and semiempirical SCF-MO package. (a) *Version 2.6 Rev. 35*; February 29, 2008; (b) *Version 2.8.0.1*; University of Bonn: Bonn, Germany, December 12, 2010; http://www.thch.ini-bonn.de/tc/orca.
47. Frisch, M. J.; Trucks, G. W.; Schlegel, H. B.; Scuseria, G. E.; Robb, M. A.; Cheeseman, J. R.; Montgomery, J. A., Jr.; Vreven, T.; Kudin, K. N.; Burant, J. C.; Millam, J. M.; Iyengar, S. S.; Tomasi, J.; Barone, V.; Mennucci, B.; Cossi, M.; Scalmani, G.; Rega, N.; Petersson, G. A.; Nakatsuji, H.; Hada, M.; Ehara, M.; Toyota, K.; Fukuda, R.; Hasegawa, J.; Ishida, M.; Nakajima, T.; Honda, Y.; Kitao, O.; Nakai, H.; Klene, M.; Li, X.; Knox, J. E.; Hratchian, H. P.; Cross, J. B.; Bakken, V.; Adamo, C.; Jaramillo, J.; Gomperts, R.; Stratmann, R. E.; Yazyev, O.; Austin, A. J.; Cammi, R.; Pomelli, C.; Ochterski, J. W.; Ayala, P. Y.; Morokuma, K.; Voth, G. A.; Salvador, P.; Dannenberg, J. J.; Zakrzewski, V. G.; Dapprich, S.; Daniels, A. D.; Strain, M. C.; Farkas, O.; Malick, D. K.; Rabuck, A. D.; Raghavachari, K.; Foresman, J. B.; Ortiz, J. V.; Cui, Q.; Baboul, A. G.; Clifford, S.; Cioslowski, J.; Stefanov, B. B.; Liu, G.; Liashenko, A.; Piskorz, P.; Komaromi, I.; Martin, R. L.; Fox, D. J.; Keith, T.; Al-Laham, M. A.; Peng, C. Y.; Nanayakkara, A.; Challacombe, M.; Gill, P. M. W.; Johnson, B.; Chen, W.; Wong, M. W.; Gonzalez, C.; Pople, J. A. *Gaussian® 03, Revision E.01*; Gaussian: 340 Quinnipiac St., Bldg. 40, Wallingford, CT 06492, USA, September 11, 2007.
48. Nazarski, R. B., to be published. The use of 71 test molecules gave the following preliminary TZ-level results for $CHCl_3$ solution modeled by the PCM ($CHCl_3$, Bondi) method: WC04 (r^2=0.9961, SD=2.2 ppm), WP04 (r^2=0.9994, SD=0. 33 ppm).
49. Nazarski, R. B.; Pasternak, B.; Leśniak, S. VIth Symposium on: Nuclear Magnetic Resonance in Chemistry, Physics and Biological Sciences, Warsaw, Sep 22–24, 2010, poster; Abstracts, P-35.
50. It was found with time,[48] that the standard B3LYP/6–31G(d) PCM (CHCl3, UA0) geometries are considerably easier computed than those constructed applying the radii of Bondi, i.e., following the recommendations of Wiitala et al.[15e] Accordingly, only such standard 'solvated' structures were used in this work, because the WP04 functional (used in further NMR calculations) was recently recognized[15h] as being not very sensitive to small changes in the molecular geometry.
51. (a) Grimme, S. *J. Chem. Phys.* **2006**, *124*, 034108-1–034108-16; (b) Schwabe, T.; Grimme, S. *Phys. Chem. Chem. Phys.* **2007**, *9*, 3397–3406.
52. López, C. S.; Pérez-Balado, C.; Rodríguez-Graña, P.; de Lera, Á. R. *Org. Lett.* **2008**, *10*, 77–80.
53. An identical scale factor of 0.97 was used at a very similar B3LYP/TZV2P level.[45b,51]
54. Koskowich, S. M.; Johnson, W. C.; Paley, R. S.; Rablen, P. R. *J. Org. Chem.* **2008**, *73*, 3492–3496.
55. All required equations and parameters are implemented in a versatile Java applet available online at http://www-jmg.ch.cam.ac.uk/tools/nmr/DP4.
56. Riveira, M. J.; Gayathri, C.; Navarro-Vázquez, A.; Tsarevsky, N. V.; Gil, R. R.; Mischne, M. P. *Org. Biomol. Chem.* **2011**, *9*, 3170–3175.
57. *PCMODEL V 8.5, Molecular Modeling Software for Windows Operating System, Apple Macintosh OS, Linux and Unix*; Serena Software: Box 3076, Bloomington, IN 47402–3076, USA, August 2003.

58. (a) Saunders, M. *J. Am. Chem. Soc.* **1987**, *109*, 3150–3152; (b) Saunders, M.; Houk, K. N.; Wu, Y.-D.; Still, W. C.; Lipton, M.; Chang, G.; Guida, W. C. *J. Am. Chem. Soc.* **1990**, *112*, 1419–1427 and refs therein.
59. (a) Lii, J.-H.; Allinger, N. L. *J. Comput. Chem.* **1991**, *12*, 186–199; (b) Midland, M. M.; Asirwatham, G.; Cheng, J. C.; Miller, J. A.; Morell, L. A. *J. Org. Chem.* **1994**, *59*, 4438–4442.
60. *HyperChem: Molecular Modeling System, Release 8.0.3 for Windows*; Hypercube: Gainesville, FL 32601, USA, June 2007.
61. (a) Becke, A. D. *Phys. Rev. A* **1988**, *38*, 3098–3100; (b) Becke, A. D. *J. Chem. Phys.* **1993**, *98*, 5648–5652.
62. (a) Lee, C.; Yang, W.; Parr, R. G. *Phys. Rev. B* **1988**, *37*, 785–789; (b) Miehlich, B.; Savin, A.; Stoll, H.; Preuss, H. *Chem. Phys. Lett.* **1989**, *157*, 200–206.
63. (a) Halgreen, T. A. *J. Am. Chem. Soc.* **1992**, *114*, 7827–7843; (b) MMFFvdW. par – Van der Waals Parameters; Copyright ©Merck and Co., Inc., Rahway, New Jersey, USA, 1994, 1995, 1996. All Rights Reserved; (c) Halgreen, T. A. *J. Comput. Chem.* **1999**, *20*, 730–748 and refs therein.
64. Our initial calculations of the geometry and energy for the highly flexible conformers **A**–**C** of lactams **1**, by using the standard grid, gave rather inconsistent results on their energetics.
65. Farkas, Ö; Schlegel, H. B. *J. Chem. Phys.* **1999**, *111*, 10806–10814 and refs therein.
66. Bondi, A. *J. Phys. Chem.* **1964**, *68*, 441–451.
67. Wilson, E. B., Jr.; Decius, J. C.; Cross, P. C. *Molecular Vibrations: The Theory of Infrared and Raman Vibrational Spectra*; McGraw-Hill Book: New York, NY, 1955.
68. (a) Schäfer, A.; Huber, C.; Ahlrichs, R. *J. Chem. Phys.* **1994**, *100*, 5829–5835; (b) Weigend, F.; Ahlrichs, R. *Phys. Chem. Chem. Phys.* **2005**, *7*, 3297–3305.
69. **CAUTION**. The initially used version of ORCA[46a] had the def2-SVP and def2-TZVP basis sets erroneously implemented for the H-atom. The correct def2-TZVP basis set was downloaded from the EMSL Basis Set Library, see Ref. 22f.
70. (a) Weigend, F.; Häser, M. *Theor. Chem. Acc.* **1997**, *97*, 331–340; (b) Weigend, F.; Köhn, A.; Hättig, C. *J. Chem. Phys.* **2002**, *116*, 3175–3183.
71. (a) Weigend, F.; Häser, M.; Patzelt, H.; Ahlrichs, R. *Chem. Phys. Lett.* **1998**, *294*, 143–152; (b) All these basis sets are available for free download from ftp://ftp.chemie.uni-karlsruhe.de/pub/cbasen.
72. (a) Huzinaga, S. *J. Chem. Phys.* **1965**, *42*, 1293–1302; (b) Huzinaga, S. *Approximate Atomic Functions. Technical Report. Division of Theoretical Chemistry, Department of Chemistry*; University of Alberta: Edmonton, Canada, 1971.
73. Nazarski, R. B. *Phosphorus, Sulfur Silicon* **2009**, *184*, 1036–1046.
74. Alcântara, A. F. C.; Piló-Veloso, D.; De Almeida, W. B.; Maltha, C. R. A.; Barbosa, L. C. A. *J. Mol. Struct.* **2006**, *791*, 180–185.
75. Zakai, U. I.; Błoch-Mechkour, A.; Jacobsen, N. E.; Abrell, L.; Lin, G.; Nichol, G. S.; Bally, T.; Glass, R. S. *J. Org. Chem.* **2010**, *75*, 8363–8371.